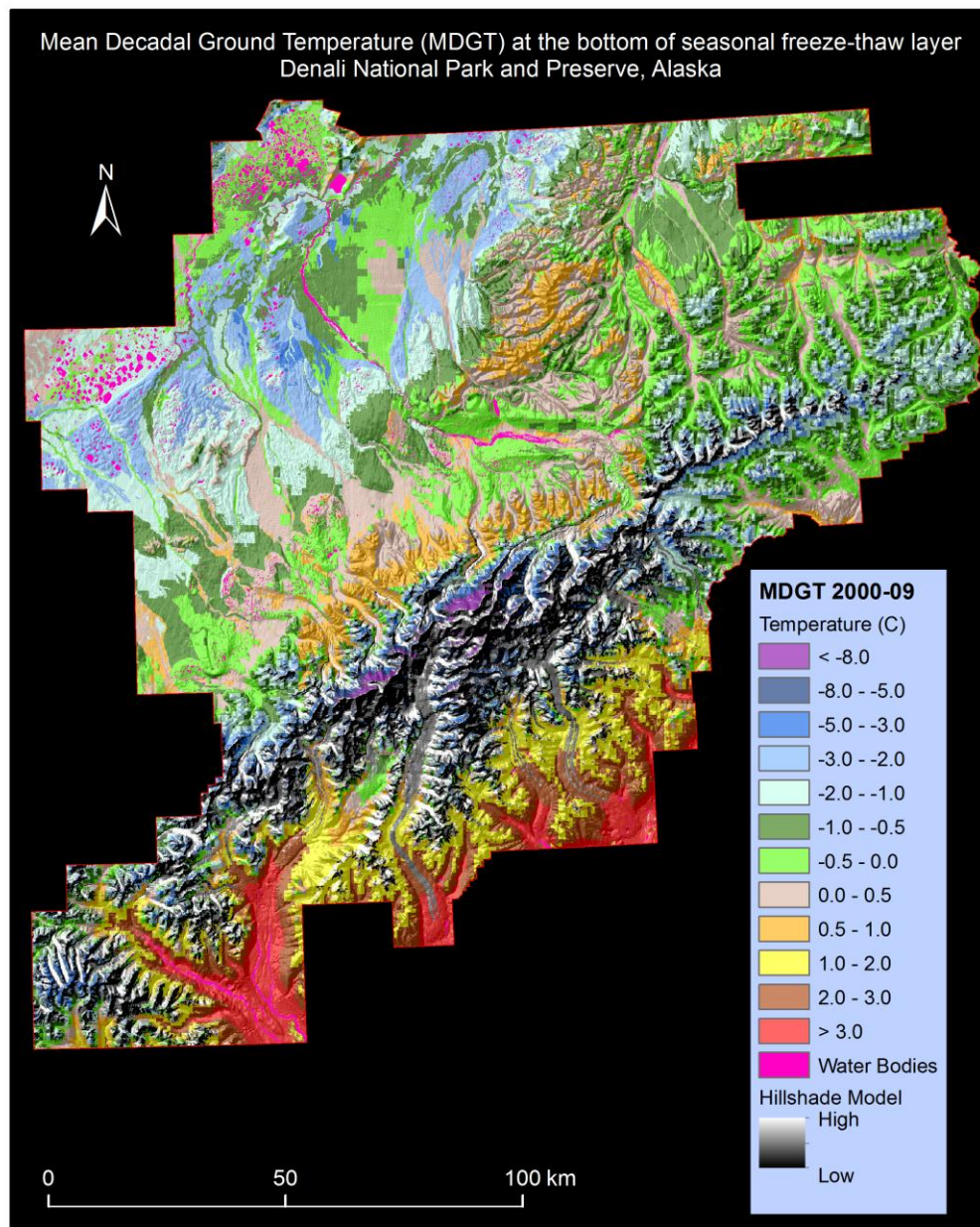




# High-Resolution Permafrost Modeling in Denali National Park and Preserve

Natural Resource Technical Report NPS/CAKN/NRTR—2014/858



**ON THE COVER**

Permafrost map of Denali National Park and Preserve, Alaska. The negative temperature values, shown in shades of green and blue, indicate presence of near-surface permafrost. The positive temperature values, shown in shades of brown and red, indicate absence of near-surface permafrost. The acronym MDGT stands for Mean Decadal Ground Temperature. The MDGT map is draped over a hillshade model shown in grayscale. The hillshade model is apparent in places where snow-ice landcover class is masked out.

Image courtesy of S. Panda.

---

# High-Resolution Permafrost Modeling in Denali National Park and Preserve

Natural Resource Technical Report NPS/CAKN/NRTR—2014/858

Santosh K. Panda  
Sergey S. Marchenko  
Vladimir E. Romanovsky

Geophysical Institute  
University of Alaska Fairbanks  
903 Koyukuk Drive  
Fairbanks, Alaska 99775

March 2014

U.S. Department of the Interior  
National Park Service  
Natural Resource Stewardship and Science  
Fort Collins, Colorado

The National Park Service, Natural Resource Stewardship and Science office in Fort Collins, Colorado, publishes a range of reports that address natural resource topics. These reports are of interest and applicability to a broad audience in the National Park Service and others in natural resource management, including scientists, conservation and environmental constituencies, and the public.

The Natural Resource Technical Report Series is used to disseminate results of scientific studies in the physical, biological, and social sciences for both the advancement of science and the achievement of the National Park Service mission. The series provides contributors with a forum for displaying comprehensive data that are often deleted from journals because of page limitations.

All manuscripts in the series receive the appropriate level of peer review to ensure that the information is scientifically credible, technically accurate, appropriately written for the intended audience, and designed and published in a professional manner. This report received informal peer review by subject-matter experts who were not directly involved in the collection, analysis, or reporting of the data.

Views, statements, findings, conclusions, recommendations, and data in this report do not necessarily reflect views and policies of the National Park Service, U.S. Department of the Interior. Mention of trade names or commercial products does not constitute endorsement or recommendation for use by the U.S. Government.

This report is available in digital format from the Natural Resource Publications Management website (<http://www.nature.nps.gov/publications/nrpn/>). To receive this report in a format optimized for screen readers, please email [irma@nps.gov](mailto:irma@nps.gov).

Please cite this publication as:

Panda, S. K., S. S. Marchenko, and V. E. Romanovsky. 2014. High-resolution permafrost modeling in Denali National Park and Preserve. Natural Resource Technical Report NPS/CAKN/NRTR—2014/858. National Park Service, Fort Collins, Colorado.

# Contents

|   | Page |
|---|------|
| Figures.....  | v    |
| Tables.....   | vi   |
| Executive Summary .....   | vii  |
| Acknowledgments.....  | ix   |
| List of Acronyms .....  | ix   |
| 1. Introduction.....  | 1    |
| 2. Denali National Park and Preserve (DENA).....  | 3    |
| 3. GIPL 1.0 Model .....   | 6    |
| 3.1. GIPL 1.0 Model Input .....   | 6    |
| 3.1.1. Climate Data.....  | 6    |
| 3.1.2. Ecotype Data .....   | 6    |
| 3.1.3. Soil Data .....  | 7    |
| 3.1.4. Snow Data .....  | 7    |
| 3.2. GIPL 1.0 Model Output.....   | 8    |
| 4. Preparation of Input Data for Modeling.....  | 9    |
| 4.1. Ice-Water Mask .....   | 9    |
| 4.2. Replacing ‘Shadow’ and ‘Cloud’ Pixels of the Landcover Map with Proxy<br>Landcover Classes ..... | 9    |
| 4.3. Climate Forcing.....   | 9    |
| 4.4. Ecotype Map.....   | 10   |
| 4.5. Soil Landscape Map .....   | 10   |
| 4.6. Snow Map.....  | 10   |
| 5. Results.....   | 12   |
| 5.1. CRU Climate Forcing (1950-1959 and 2000-2009).....   | 12   |
| 5.2. 5-GCM Composite Climate Forcing (2001-2010, 2051-2060, and 2091-2100).....                       | 17   |

# Contents (continued)

|   | Page |
|---|------|
| 5.3. Accuracy Assessment.....   | 24   |
| 5.3.1. Warm-biased Test.....  | 24   |
| 5.3.2. Cold-biased Test.....  | 25   |
| 5.3.3. Comparison with Recorded Ground Temperature.....   | 25   |
| 6. Deliverables .....   | 29   |
| 7. Literature Cited .....   | 30   |
| Appendix A. Tables of Landcover Classes, Landtype Associations, and Snow Classes.....   | 33   |
| Appendix B. The GIPL Model for Estimation of Temporal and Spatial Variability of the Active-Layer Thickness and Mean Annual Ground Temperatures ..... | 41   |

# Figures

|   | Page |
|---|------|
| <b>Figure 1.</b> Location of Denali National Park and Preserve (DENA) in Alaska.....  | 4    |
| <b>Figure 2.</b> Ecomap of DENA.....  | 5    |
| <b>Figure 3.</b> Permafrost map (1950-1959 CRU climate forcing) of Denali National Park and Preserve, Alaska.....   | 13   |
| <b>Figure 4.</b> Active-layer and seasonally-frozen-layer thickness map (1950-1959 CRU climate forcing) of Denali National Park and Preserve, Alaska. ....    | 14   |
| <b>Figure 5.</b> Permafrost map (2000-2009 CRU climate forcing) of Denali National Park and Preserve, Alaska.....   | 15   |
| <b>Figure 6.</b> Active-layer and seasonally-frozen-layer thickness map (2000-2009 CRU climate forcing) of Denali National Park and Preserve, Alaska. ....    | 16   |
| <b>Figure 7.</b> Permafrost map (2001-2010 5-GCM climate forcing) of Denali National Park and Preserve, Alaska. ....  | 18   |
| <b>Figure 8.</b> Active-layer and seasonally-frozen-layer thickness map (2001-2010 5-GCM climate forcing) of Denali National Park and Preserve, Alaska. ....  | 19   |
| <b>Figure 9.</b> Permafrost map (2051-2060 5-GCM climate forcing) of Denali National Park and Preserve, Alaska.....   | 20   |
| <b>Figure 10.</b> Active-layer and seasonally-frozen-layer thickness map (2051-2060 5-GCM climate forcing) of Denali National Park and Preserve, Alaska. .... | 21   |
| <b>Figure 11.</b> Permafrost map (2091-2100 5-GCM climate forcing) of Denali National Park and Preserve, Alaska.....  | 22   |
| <b>Figure 12.</b> Active-layer and seasonally-frozen-layer thickness map (2091-2100 5-GCM climate forcing) of Denali National Park and Preserve, Alaska. .... | 23   |
| <b>Figure 13.</b> Locations of three climate stations plotted on a Denali National Park and Preserve Hillshade Model. ....                                    | 28   |

## Tables

|  | Page |
|--|------|
| <b>Table 1.</b> Summary statistics of climate and modeled permafrost characteristics in Denali National Park and Preserve using CRU climate forcing.....   | 17   |
| <b>Table 2.</b> Summary statistics of climate and modeled permafrost characteristics in Denali National Park and Preserve using 5-GCM composite climate forcing. ....  | 24   |
| <b>Table 3.</b> Comparison of recorded air and ground temperatures at the NPS climate stations with CRU air temperature and modeled temperature at the ground surface and bottom of seasonal freeze-thaw layer. .... | 27   |

## Executive Summary

We used the CRU (1950-1959 and 2000-2009) and projected 5-GCM composite (2001-2010, 2051-2060, and 2091-2100) decadal climate forcing, ecotype (Stevens 2001), soil landscape (Clark and Duffy 2006), and snow (unpublished) maps of DENA to model the presence or absence of near-surface permafrost, temperature at the bottom of seasonal freeze-thaw layer and its thickness within DENA. We produced permafrost temperature, and active-layer and seasonally-frozen-layer thickness distribution maps through this modeling effort at a pixel spacing of 28 m. This is an immense improvement over the spatial resolution of existing permafrost maps on any part of Alaska, whether produced through the spatially explicit thermal modeling of ground temperatures or by visual interpretation of satellite images/ aerial photos using indirect surface evidences of permafrost or by compilation of information from detailed field soil/geology/ecotype surveys. The model predicted 'stable' near-surface permafrost under 49% of DENA total area during decade 2000s and its distribution is predicted to decline to 6% by 2050s and 1% by 2090s (Figure i), i.e., near-surface permafrost is predicted to be degrading in the entire DENA and completely degraded in some part of it toward the end of the century. Only tiny areas on the north-facing slopes of high mountains are predicted to have 'stable' near-surface permafrost. The accuracy tests of the modeled permafrost, and active-layer and seasonally-frozen-layer thickness maps by comparing them against the field observations of permafrost presence/absence and thaw depth (at 1375 sites within DENA) suggested 86% agreement.

We compiled the available ground temperature data from three climate stations within DENA and compared them to the modeled ground temperatures (Table 3). We attributed the air temperature differences between climate stations and the CRU data (input climate forcing) to the difference in scale of these datasets. The difference between recorded near-surface ground temperatures (at 0.02 m) and modeled ground surface temperatures at the three climate stations were smaller ( $<1^{\circ}\text{C}$ ). We attributed these differences in temperatures to three major factors: difference in scale, ground condition, and snow depth.

The GIPL 1.0 model performs competently for DENA and provides reliable permafrost temperature status for different time-periods. As we used past and projected future climate forcing for modeling, the output permafrost maps show the impact of changing climate on near-surface permafrost temperature and its distribution. These permafrost maps will facilitate the park managers to understand the current status of near-surface permafrost within DENA and how it may evolve in the future with changing climate, also to identify (vulnerable) sites at higher risk of permafrost thawing, with concurrent changes in wildlife habitats and populations. These maps will enable the park managers and decision makers to make informed decision on resource management and design of monitoring programs. Nonetheless, our model is limited in its ability to incorporate temporal changes in vegetation dynamics which could affect near-surface permafrost dynamics. Though we assumed no change in vegetation dynamics for our modeling time periods, the natural disturbances like forest fires and flooding could alter the vegetation structure and composition and consequently the ecotype at the disturbed sites resulting in reduced model prediction accuracy at those sites in the future.

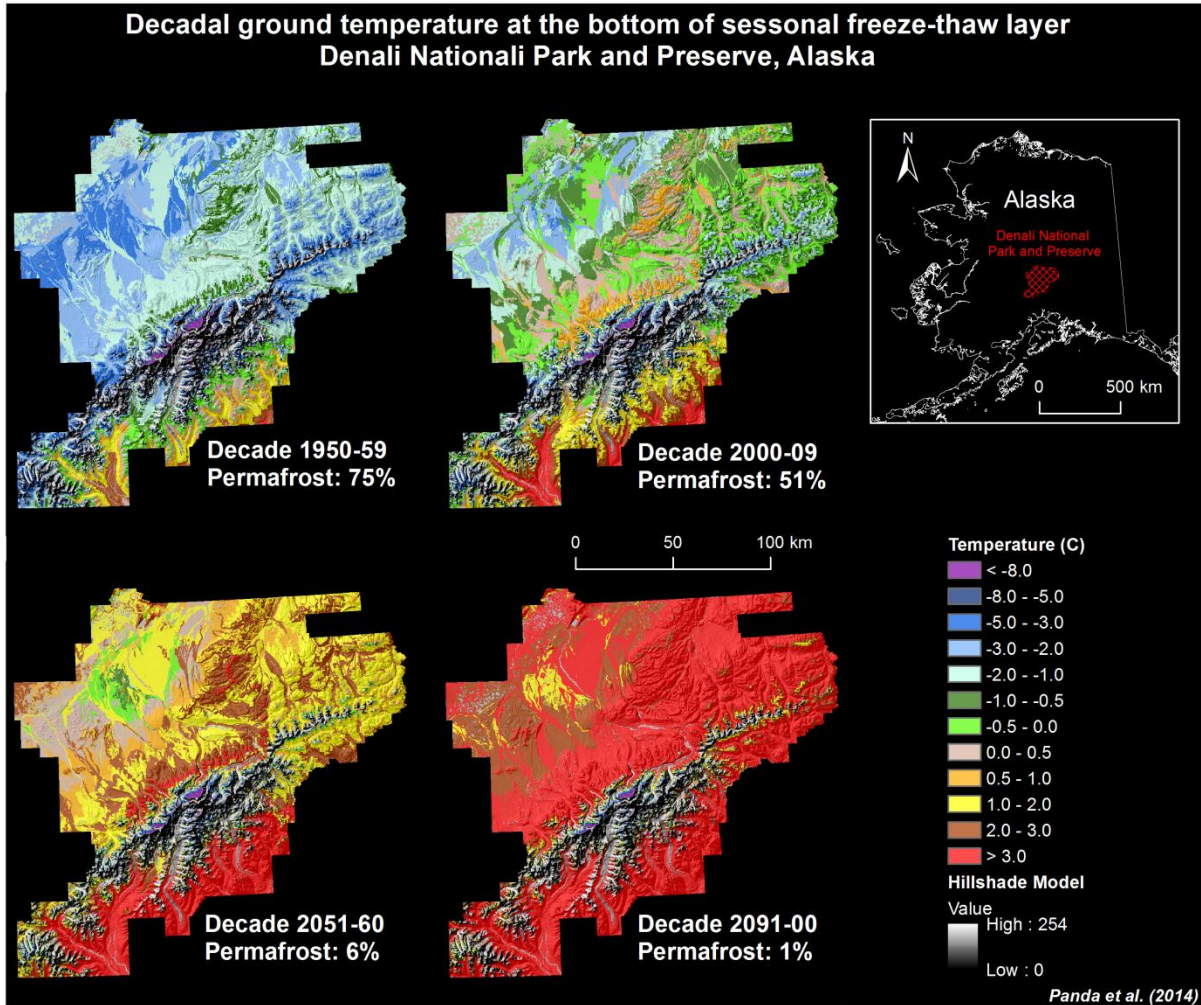


**Figure i.** Comparison of modeled permafrost maps (CRU forcing: 1950s and 2000s; 5-GCM forcing: 2050s and 2090s) of Denali National Park and Preserve. The negative temperature values, shown in shades of green and blue, indicate presence of near-surface permafrost. The positive temperature values, shown in shades of brown and red, indicate absence of near-surface permafrost. The permafrost maps are draped over hillshade model shown in gray scale. The hillshade model is apparent in places where snow-ice landcover class is masked out.

## Acknowledgments

We would like to offer our special thanks to David K Swanson for his valuable advice, support and overall management of this project. His enthusiasm for the project and willingness to give time generously has been very much appreciated. We would also like to thank Pam Sousanes for help in accessing National Park Services climate data, and Louise Farquharson and Prajna Regmi for reviewing the report and their valuable feedback.

## List of Acronyms

|       |   |
|-------|---|
| ALT   | Active-layer thickness  |
| CRU   | Climatic Research Unit  |
| DENA  | Denali National Park and Preserve   |
| GCM   | Global climate models   |
| MAGST | Mean annual ground surface temperature                                      |
| MAGT  | Mean annual ground temperature at the bottom of seasonal freeze-thaw layer  |
| MDGT  | Mean decadal ground temperature at the bottom of seasonal freeze-thaw layer |
| NPS   | National Park Service   |
| SFLT  | Seasonally-frozen-layer thickness   |
| SNAP  | Scenario Network for Alaska & Arctic Planning                               |



# 1. Introduction

Permafrost is defined as “ground (soil or rock and included ice and organic material) that remains at or below 0°C for at least two consecutive years, for natural climatic reasons” (van Everdingen 1998). Permafrost and permafrost-affected regions underlie ~22% of the exposed land in the Northern hemisphere (Brown et al. 1997) and ~80% of Alaska (Jorgenson et al. 2008). Permafrost terrain consists of an “active layer” at the surface that thaws in summer and freezes again in winter (Muller 1947). The active layer is critical to the ecology and hydrology of permafrost terrain as it provides a rooting zone for plants and acts as a seasonal aquifer for near-surface ground water (Burn 1998). Its thickness is highly variable and can be anywhere from a few decimeters to several meters, depending on the local microclimatic condition, topography, local hydrology, thickness of surface organic layer, vegetation type, and winter snow condition. Similarly, the form and texture of ground ice within permafrost also varies greatly. Ground ice forms include thin lenses of ice, layered ice, reticulated vein ice, and ice wedges as big as 2-4 m long and 3-5 m deep (French and Shur 2010, Kanevskiy et al. 2011).

Permafrost is pervasive in Alaska’s National Parks, Preserves, and Monuments. Nearly 40 million acres of Alaska’s National Park Service (NPS) units lie within the zone of continuous or discontinuous permafrost. This area constitutes over 70% of Alaska’s NPS land and nearly half of all the NPS administered land in the US. Much of this permafrost is vulnerable to major changes due to climatic warming because 1) it has temperatures within a few degrees of freezing, such that relatively minor warming could destabilize it entirely, and/or 2) it contains ice-rich material near the surface that could thaw with climatic warming, leading to major reconfiguration of the landscape through the development of thermokarst (an irregular topography resulting from melting of excess ground ice). Thawing of permafrost could have many consequences, such as drainage of thermokarst lakes, creation of new thaw ponds, soil erosion, thaw slumps, increased sediment loads and siltation of streams and lakes, release of greenhouse gasses, and changes in soil wetness and nutrient cycling. Thawing permafrost is second only to wildfires as a major disturbance to boreal forests (Jorgenson and Osterkamp 2005). Permafrost has been identified by the Arctic and Central Alaska Network as one of the “vital signs” of ecosystem health in Alaska’s national parks (MacCluskie and Oakley 2005, Lawler et al. 2009).

Permafrost is a subsurface feature that is difficult to observe and map directly. Temperature measurements are required to determine the status of permafrost and warming permafrost is in danger of thawing (Osterkamp and Jorgenson 2009). Existing information about the distribution and temperature of permafrost in NPS units is limited due to the lack of borehole observations on NPS lands. Modeling of permafrost distribution has proven very useful for extrapolating between widely spaced boreholes where direct observations are made. Permafrost distribution and the thickness of the active layer can be modeled, given sufficient data about soil and ground properties, vegetation, topography, atmospheric climate, and soil temperatures. The same models used to map current permafrost distribution and active-layer thickness can be used to predict the future state of permafrost by using projected climate forcing and scenarios.

Geophysical Institute Permafrost Laboratory (GIPL) at University of Alaska Fairbanks has developed a model, “GIPL 1.0 - Spatially Distributed Model of Permafrost Dynamics in Alaska”, that has successfully mapped permafrost distribution and active-layer thickness (ALT) at kilometer scale for the State of Alaska (Marchenko et al. 2008). The GIPL 1.0 model gives a good representation of the coupling between permafrost and the atmosphere. It shows an accuracy of  $\pm 0.2 - 0.4^{\circ}\text{C}$  for the mean annual ground temperature and  $\pm 0.1 - 0.3$  m for the active-layer thickness calculations when applied to long-term (decadal and longer time scale) averages (Sazonova and Romanovsky 2003). As a part of its inventory and monitoring program, the NPS has obtained or is in the process of gathering data that can be used to make improved runs of the GIPL 1.0 model for NPS units in Alaska.

The goal of this project is to facilitate cooperation between NPS and GIPL to obtain improved and higher-resolution maps for NPS lands of permafrost distribution, temperature, and active-layer thickness under various climate scenarios, including present conditions, the recent past (e.g., 1950, prior to recently observed warming), and the future. The NPS environmental data (soil landscape and ecotype maps) along with past and projected climate forcing and scenarios from global climate datasets are used to create maps of near-surface permafrost distribution and its temperature, and active-layer thickness, for the recent past (1950s), the present (2000s), and the future (2050s and 2090s). Field observation of permafrost presence/absence, summer thaw depth, and ground temperature records from NPS climate stations are used to assess the overall accuracy of the modeled permafrost maps.

## 2. Denali National Park and Preserve (DENA)

The DENA occupies 6.06 million acres of land in interior and southcentral Alaska (Figure 1). It is well known for Mt. McKinley (the highest mountain in North America), the Alaska Range, the scenic and unspoiled beauty of the landscape, and the wildlife that inhabits the parks (<http://science.nature.nps.gov/im/units/cakn/DENA.cfm>).

DENA includes five major physiographic sections, namely Alaska Mountains, South Central Mountains, Yukon-Kuskokwim Bottomlands, Kuskokwim Mountains, and Cook Inlet Lowlands (Nowacki and Brock 1995; Figure 2). The Alaska Range includes both the Alaska Mountains and South Central Mountains sections and occupies ~60% of the park. These mountain ranges are capped by permanent snowfields and glaciers. Alpine glacial plains skirt the mountains along DENA's north side, gradually giving way to lowland forested plains and hills, a land underlain by permafrost and modified by wildfire (Clark and Duffy 2006). The Yukon-Kuskokwim Bottomlands section, located in the northwestern part of DENA, consists of an expansive lowland area of plains, hills, relict sand dunes, bogs, fens, and ponds. This section represents the largest contiguous area of permafrost-affected soils, as well as wetlands within DENA. The Kuskokwim Mountains and Cook Inlet Lowland sections together occupy less than 10% of DENA; the former is underlain by continuous and discontinuous permafrost whereas the latter is completely devoid of permafrost.

Almost 17% of DENA is unvegetated ice and rocky mountain slopes. There are two major vegetation types or biomes within the park, taiga and tundra. Taiga or boreal forest can be found at lower elevations (<2,700 feet). Above 2,700 feet, taiga gives way to tundra. There are two general types of tundra found in DENA – dry tundra and moist tundra – with gradations in between.

DENA is divided into two sub-regional climates. Areas north of the hydrographic divide of the Alaska Range are considered sub-arctic continental, referred to as Interior, and those lying to the south are transitional maritime-continental, referred to as South Central. Permafrost is common throughout the Interior climatic zone and generally absent in the South Central climatic zone. Permafrost is extensive within loamy textured soils of the Alaska Mountains, Yukon-Kuskokwim Plain, and Kuskokwim Mountains sections (Clark and Duffy 2006).

Permafrost distribution can be classified as continuous (>90% of land area underlain by permafrost), discontinuous (90% – 50%), sporadic (50% – 10%), or isolated (<10%) (Ferrians 1965). In DENA, permafrost distribution ranges from areas of continuous permafrost (which contains some of the southern-most coldest permafrost in North America) to areas devoid of permafrost (Adema 2006). Nonetheless, the best permafrost information available to date for DENA is the limited point observations, and the soil survey map by Clark and Duffy (2006). Up-to-date and comprehensive spatial information on the state of permafrost is presently lacking and consequently the vulnerability of permafrost and DENA landscape to climate change is unknown. Some recent borehole temperature measurements showed significant permafrost warming throughout Alaska since the 1980s (Osterkamp 2007, Romanovsky et al. 2010a, 2010b). Thawing permafrost and thermokarst terrain have also been observed within and near park boundary (Adema 2006, Yocum 2006, Schuur 2008, Osterkamp et al. 2009). Permafrost is the physical foundation on which the ecosystems in the

park rest and thawing of ice-rich permafrost alters this foundation. Permafrost thaw has the potential to greatly alter ecosystems and their net carbon balance i.e., the difference between carbon uptake and emission. In lowlands, a shift from boreal forests to shrubby wetlands or grasslands often occurs with concurrent changes in wildlife populations (Jorgenson et al. 2001). Tracking the distribution and condition of permafrost and development of thermokarst within DENA will provide information about one of the most important drivers of landscape change in the 21st century (<http://science.nature.nps.gov/im/units/cakn/vitalsign.cfm?vsid=43>).

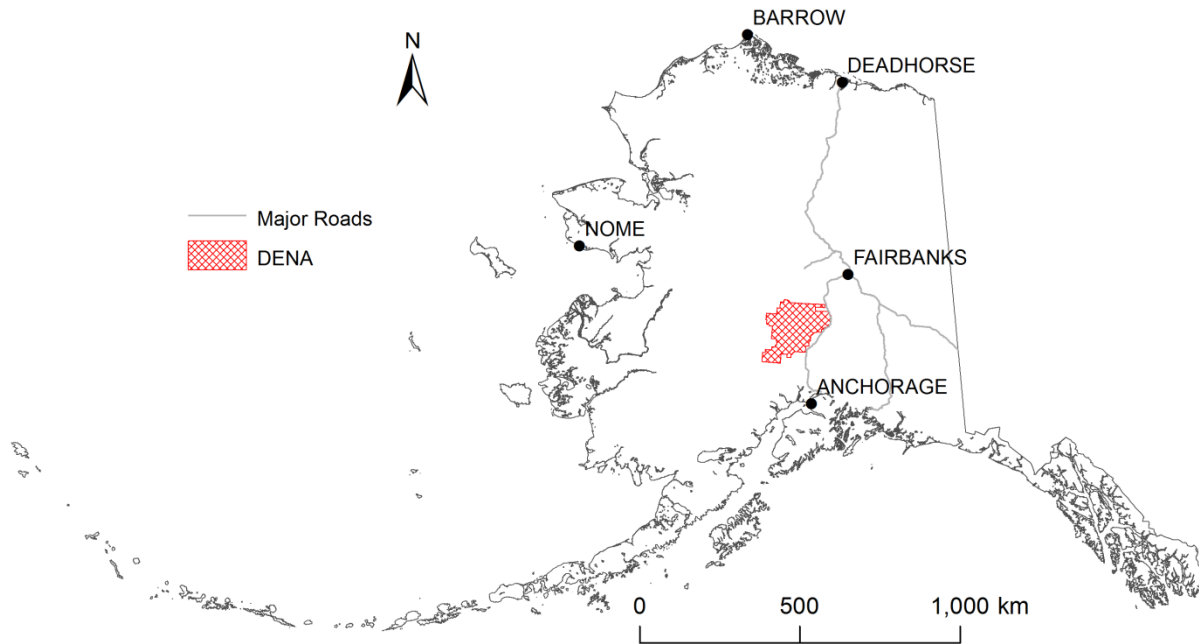


**Figure 1.** Location of Denali National Park and Preserve (DENA) in Alaska.

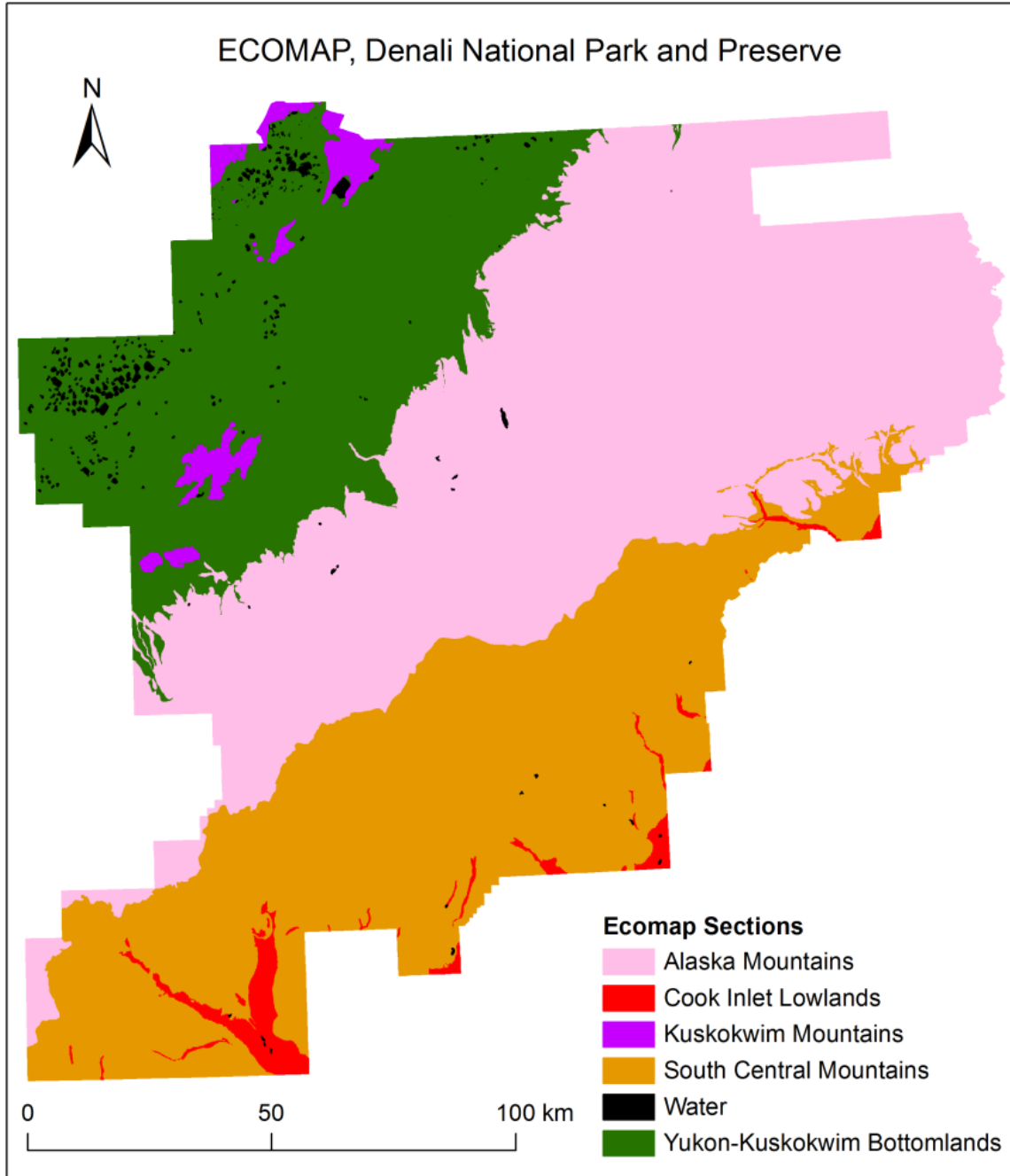


**Figure 2.** Ecomap of DENA. DENA is divided into 5 ecomap sections and 22 ecomap subsections (ECOMAP 1993, Nowacki and Brock 1995).

### 3. GIPL 1.0 Model

GIPL 1.0 is a quasi-transitional, spatially distributed, equilibrium model for calculating the mean annual temperature at the ground surface and bottom of seasonal freeze-thaw layer and thickness of seasonal freeze-thaw layer. In the absence of permafrost the seasonal freeze-thaw layer is called “seasonally-frozen layer” (the top layer of the ground that freezes in winter and thaws back in summer and does not have permafrost underneath). The model accounts for the effects of snow cover, surface vegetation, soil moisture, and soil thermal properties (Figure B1). Refer to Appendix B for detailed description of this model.

#### 3.1. GIPL 1.0 Model Input

##### 3.1.1. *Climate Data*

We used historical (1901–2009) monthly average air temperature (°C) and total precipitation (mm) data, CRU TS 3.1 from the University of East Anglia (UK) Climatic Research Unit, downscaled to 771 m by Scenario Network for Alaska & Arctic Planning (SNAP) for past climate forcing (SNAP 2012). Projected (2001–2100) monthly average air temperature (°C) and total precipitation (mm) data are available from Fourth Assessment Report (AR4) Global Climate Models (GCM) for a range of possible emission scenarios. Walsh et al. (2008) identified 5 out of a set of 15 global models used in the Coupled Model Intercomparison Project (CMIP) as best performer for Alaska and Greenland. Those 5 AR4 GCMs are:

- *cccma\_cgcm31*: Canadian Centre for Climate Modeling and Analysis, Coupled General Circulation Model version 3.1 – t47, Canada
- *mpi\_echam5*: Max Planck Institute for Meteorology, European Centre Hamburg Model 5, Germany
- *gfdl\_cm21*: Geophysical Fluid Dynamics Laboratory, Coupled Model 2.1, United States
- *ukmo\_hadcm3*: UK Met Office – Hadley Centre, Coupled Model version 3.0, United Kingdom
- *miroc3\_2\_medres*: Center for Climate System Research, Model for Interdisciplinary Research on Climate 3.2 (medres), Japan

SNAP averaged the monthly average air temperature and total precipitation projections from the above 5 models for 3 possible emission scenarios (B1: low, A1B: moderate, and A2: high) and created a composite climate dataset for Alaska downscaled to 771 m (SNAP 2012). We used this 5-GCM composite climate dataset for A1B emission scenario as the future climate forcing for the GIPL 1.0 model runs.

##### 3.1.2. *Ecotype Data*

Landcover mapped by Stevens et al. (2001) are used as ecotype model input. They mapped 25 landcover classes at intermediate scales (1:63,360 – 1:100,000), following a modified version of the Alaska Vegetation Classification system at levels III and IV (Vioreck et al. 1992), using Landsat

Thematic Mapper (TM) multi-spectral imagery as the primary data source and SPOT XS data as the secondary source.

Surface organic layer thickness and its thermal diffusivity are the two essential ecotype parameters required for ground temperature modeling. Both of these parameters are not available for DENA ecotypes and are thus prescribed. We prescribed surface organic layer thickness based on the vegetation types and their site characteristics in each landcover unit and thermal diffusivity values based on our modeling experience in other parts of Alaska. The following ecotype properties are used as the model input (Table A1):

- Thawed thermal diffusivity ( $\text{m}^2/\text{s}$ )
- Frozen thermal diffusivity ( $\text{m}^2/\text{s}$ )
- Surface organic layer thickness (m)

### **3.1.3. Soil Data**

One hundred-and-fifty-two landtype associations are identified within DENA (Clark and Duffy 2006). Landtype associations are groupings of landtypes based on similarities in geomorphic process, geologic rock types, soil complexes, and vegetation communities. Each landtype association represents a repeatable pattern of landforms, soil complexes, and vegetation communities that can be consistently delineated on maps. Primary criteria used to delineate and name landtype associations included major biome and landforms. Additional criteria used included lithology of soil parent material, relative wetness, and other landscape features like permafrost distribution (Clark and Duffy 2006). We used the landtype association map as soil map model input. We prescribed the following thermal properties to each landtype association as the model input (Yershov 1984; Table A2):

- Thawed heat capacity ( $\text{J}/\text{m}^3\text{K}$ )
- Frozen heat capacity ( $\text{J}/\text{m}^3\text{K}$ )
- Thawed thermal conductivity ( $\text{W}/\text{m}\cdot\text{K}$ )
- Frozen thermal conductivity ( $\text{W}/\text{m}\cdot\text{K}$ )
- Volumetric water content (Fraction of 1)

### **3.1.4. Snow Data**

Snow cover plays an important role in the heat exchange processes between the land surface and the atmosphere. The insulating effect of the snow cover has been calculated using approximate formulas derived by Lachenbruch (1959) and Romanovsky (1987) which incorporate ground properties, vegetation cover, and their respective effect on heat turnovers through the snow. Heat turnovers are defined as the quantity of incident heat (during the heating period), or out-going heat (during the cooling period) throughout the medium over a given time interval (usually half year increments). The model takes into account only conductive heat transfer through different mediums.

We created a snow map of Alaska by combining the five seasonal snow classes identified by Sturm et al. (1995) with ecotypes from North America Land Cover Characteristics Data Base Version 2.0 (Loveland et al. 1999). Sturm et al. (1995) defined each snow class by a unique ensemble of the physical properties of the snow (depth, density, thermal conductivity, number of layers, and degree of wetting). Ecotypes in the North America Land Cover Characteristics Data Base Version 2.0 are mapped using multi-temporal AVHRR data and other ancillary data sets. The Alaska snow map has twelve classes (this is an unpublished part of the GIPL model) and nine of those snow classes are present in DENA. The following snow properties are used as the model input (Table A3):

- Density of fresh snow ( $\text{kg/m}^3$ )
- Maximum density of snow ( $\text{kg/m}^3$ )

### **3.2. GIPL 1.0 Model Output**

The GIPL 1.0 permafrost model calculates the following permafrost characteristics:

- Mean annual ground surface temperature (MAGST,  $^{\circ}\text{C}$ ).
- Mean annual ground temperature (MAGT,  $^{\circ}\text{C}$ ) at the bottom of seasonal freeze-thaw layer.
- Thickness (m) of seasonal freeze-thaw layer.

## 4. Preparation of Input Data for Modeling

The preparation of input data for the model runs was done in a GIS environment using the program ArcMap 10 ([www.esri.com/software/arcgis/arcgis-for-desktop](http://www.esri.com/software/arcgis/arcgis-for-desktop)).

### 4.1. Ice-Water Mask

We masked out the glaciers and water bodies within DENA as GIPL 1.0 model calculates temperature on and below the land surface only. We generated the Snow-Ice-Water mask by using the following procedure:

- Generated a DENA boundary shape file (DENA-Boundary.shp) from the DENA soil map developed by Clark and Duffy (2006). We used this boundary shape file to subset rest of the input data layers — air temperature, precipitation, landcover, and snow map.
- Converted the vector soil map to a raster soil map of same pixel size as the DENA landcover map (Stevens et al. 2001).
- Reclassified the water class identified in the raster soil map as ‘nodata’.
- Reclassified the snow-ice and water classes identified in the landcover map as ‘nodata’.
- Integrated the above two reclassified raster maps. The resulting raster map (Snow-Ice-Water-Mask.tif) has snow-ice and water classes identified as ‘nodata’.
- This ‘Snow-Ice-Water-Mask.tif’ raster layer was used to mask out snow-ice and water pixels from every model input data layers (i.e., air temperature, precipitation, and snow data).

### 4.2. Replacing ‘Shadow’ and ‘Cloud’ Pixels of the Landcover Map with Proxy Landcover Classes

The original DENA landcover map has a ‘shadow’ and a ‘cloud’ class identifying pixels where landcover could not be mapped due to the presence of shadow and cloud, respectively. We followed the following procedure to replace the ‘shadow’ and ‘cloud’ pixels with a proxy landcover class:

- Added a new field (landcover class) to the soil raster map attribute table. Assigned a landcover class to each soil class by looking at the dominant vegetation type of the major component of that soil class and matching it to one of the landcover classes identified within DENA.
- Reclassified the soil map as landcover map by using the assigned landcover class attribute.
- Replaced the ‘shadow’ and ‘cloud’ pixels of the original landcover map with the landcover class assigned in the previous steps.

### 4.3. Climate Forcing

The monthly average air temperature and monthly total precipitation data, from CRU TS 3.1 and 5-GCM composite, are available at 771m and 800 m cell size, respectively, for the entire state of

Alaska (SNAP 2012). We used the following procedure to prepare the input climate data for model runs:

- Created decadal average air temperature and precipitation raster layers for every month for the time periods of interest i.e., 1950-1959, 2000-2009, 2001-2010, 2051-2060, and 2091-2100.
- Created DENA subsets of the decadal average air temperature and precipitation data from the previous step by using the ‘DENA-Boundary.shp’ shape file.
- Resampled the DENA decadal average air temperature and precipitation data from the previous step to the resolution of DENA landcover map i.e., 28 m.
- Masked out the snow-ice and water pixels from the resampled decadal average air temperature and precipitation data by using ‘DENA-Snow-Ice-Water-Mask.tif’ layer.
- Used CRU air temperature data for the time periods 1950-1959 and 2000-2009. The 5-GCM composite average air temperature data for the time period 2001-2010 is 1°C colder than the CRU air temperature of 2000-2009. Since CRU data is derived from more than 3000 climate stations around the world and closer to true air temperatures than the 5-GCM air temperature, we estimated the bias between these two and applied the bias correction to the 5-GCM air temperature of 2001-2010, 2051-2060, and 2091-2100. We used the bias corrected 5-GCM air temperature data for the time periods 2001-2010, 2051-2060, and 2091-2100.
- Converted the DENA CRU air temperature, bias corrected 5-GCM average air temperature, and precipitation raster layers to ASCII format as GIPL 1.0 requires input data to be in ASCII format.

#### **4.4. Ecotype Map**

We masked out the snow-ice and water pixels from the landcover map from Section 4.2 by using ‘DENA-Snow-Ice-Water-Mask.tif’ layer. We fixed the sequence of class values by assigning a continuous sequence of numbers ‘1-20’ to the remaining landcover classes. Converted the resulting raster (.tif) landcover map to ASCII format.

#### **4.5. Soil Landscape Map**

We masked out the snow-ice and water pixels from DENA raster soil map. We reclassified the soil map in order to fix the sequence of class values. We reassigned a continuous sequence of numbers ‘1-151’ to the remaining soil classes. Converted the resulting raster (.tif) soil map to ASCII format.

#### **4.6. Snow Map**

The Alaska snow map described in Section 3.1.4 is available at 2 km spatial resolution. We used the following procedure to prepare the input DENA snow map for model runs:

- Created DENA subset of the Alaska snow map by using the ‘DENA-Boundary.shp’ shape file.

- Resampled the DENA snow map from the previous step to 28 m spatial resolution.
- Masked out the ‘snow-ice’ and ‘water’ bodies from the resampled DENA snow map by using ‘DENA-Snow-Ice-Water-Mask.tif’ layer.
- Reclassified the DENA snow map to have a continuous sequence of class values ‘1-9’, as 9 out of the 12 snow classes identified in Alaska are present within DENA.
- Converted the raster DENA snow map from the previous step to ASCII format.

## 5. Results

The modeling effort resulted in high-resolution maps for DENA of near-surface permafrost temperature, and active-layer and seasonally-frozen-layer thickness distribution for the decades 1950-1959, 2000-2009, 2001-2010, 2051-2060, and 2091-2100.

### 5.1. CRU Climate Forcing (1950-1959 and 2000-2009)

In order to understand the past permafrost distribution and changes to its characteristics between 1950s and 2000s, the modeling results using CRU climate forcing should be compared and analyzed (Table 1). The CRU (1950-1959) decadal mean air temperature within DENA ranged from - 31.2°C to 1.3°C and the mean was - 3.5°C. The CRU (1950-1959) decadal mean annual precipitation ranged from 304 to 2182 mm and the mean was 679 mm. The modeled (1950-59) permafrost temperature within DENA ranged from - 22.2 to 0°C and the mean permafrost temperature was - 2.1°C, i.e., the majority of near-surface permafrost within DENA was within 2°C of freezing (Figure 3). The modeled (1950-59) active-layer thickness ranged from 0.19 to 2.45 m and the mean was 1.1 m (Figure 4). The model mapped 75% of the DENA total area as underlain by near-surface permafrost during the 1950s. The CRU (2000-2009) mean decadal air temperature was 1.9 °C warmer than that of 1950-1959 (Table 1). Consequently, the modeled (2000-2009) mean decadal permafrost temperature was 0.9°C warmer than that of 1950-1959. The model mapped 51% of the DENA total area as underlain by near-surface permafrost during the decade of 2000s, i.e., degradation of near-surface permafrost on 24% of the DENA total area in a span of 50 years (Figure 5 & Figure 6). The percentage of most vulnerable permafrost (i.e., near-surface permafrost within a degree of freezing) within DENA increased from 8.5% of DENA total area in 1950s to 30% in 2000s. The percentage of DENA total area with active-layer thickness thinner than 1 m decreased from 38% in 1950s to 19% in 2000s.

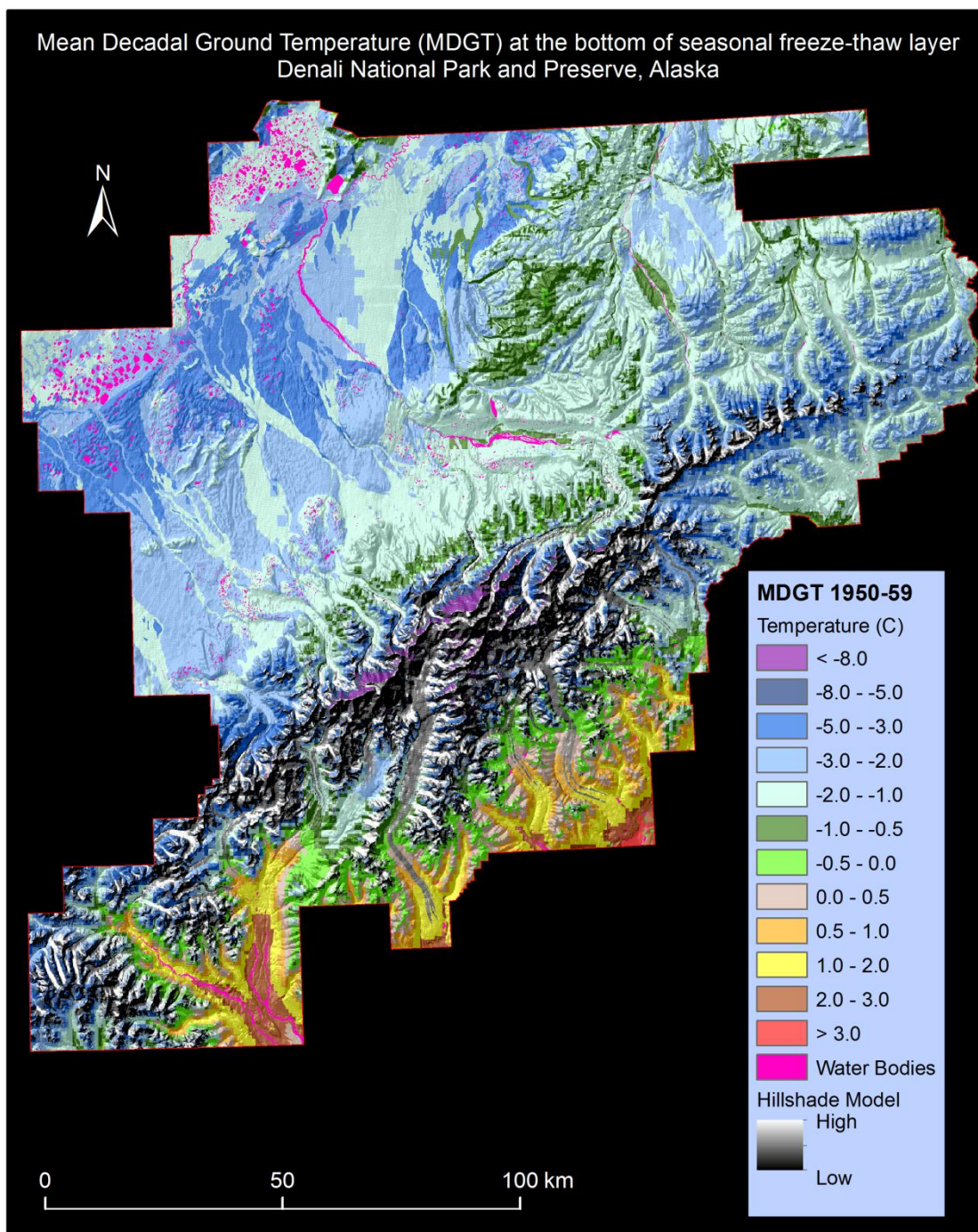


**Figure 3.** Permafrost map (1950-1959 CRU climate forcing) of Denali National Park and Preserve, Alaska. The negative temperature values, shown in shades of green and blue, indicate presence of near-surface permafrost. The positive temperature values, shown in shades of brown and red, indicate absence of near-surface permafrost. The acronym MDGT stands for Mean Decadal Ground Temperature. The MDGT map is draped over a hillshade model shown in grayscale. The hillshade model is apparent in places where snow-ice landcover is masked out.

Active-Layer Thickness (ALT) & Seasonally-Frozen-Layer (SFLT) Thickness Map  
Denali National Park and Preserve, Alaska

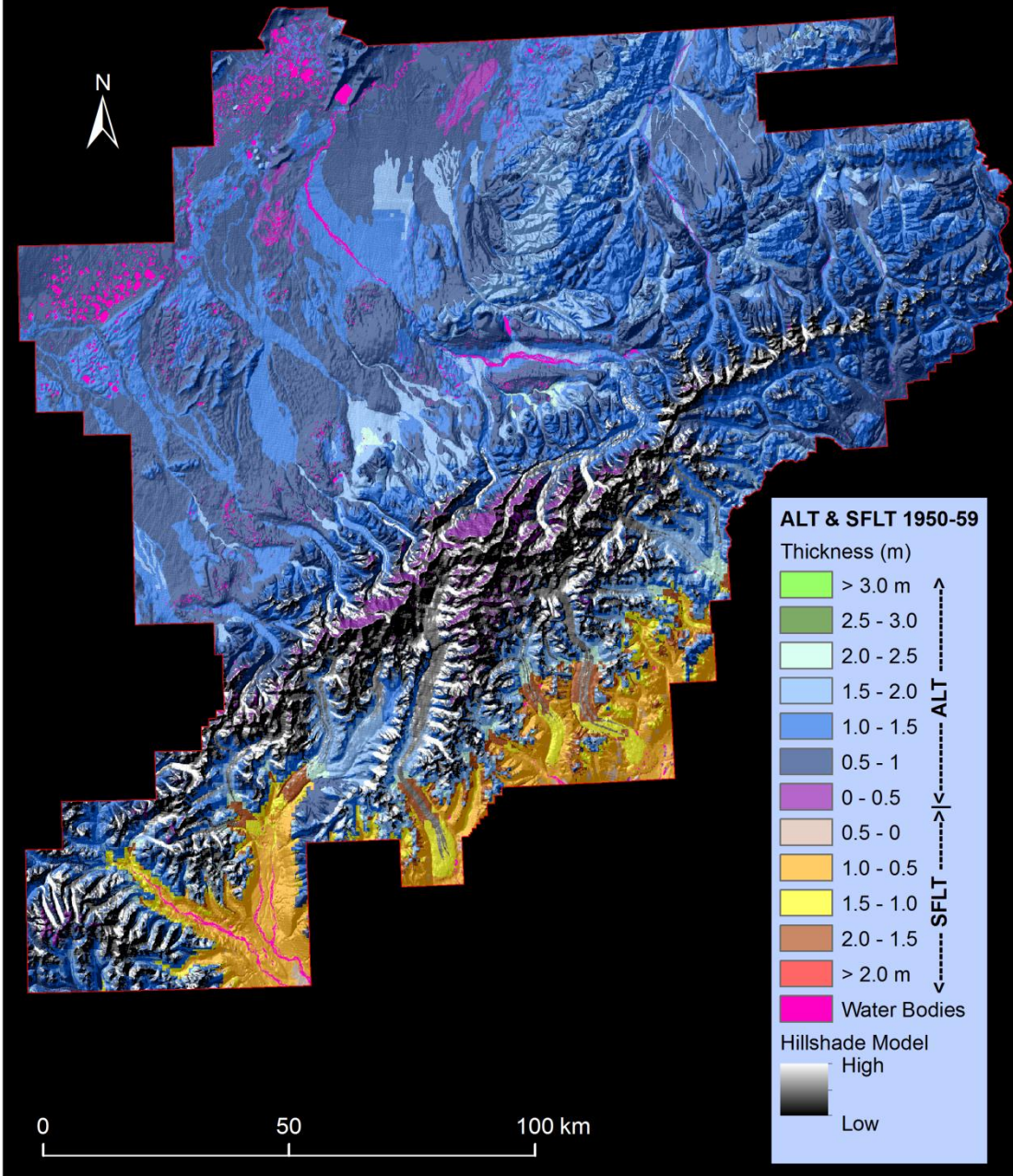


**Figure 4.** Active-layer and seasonally-frozen-layer thickness map (1950-1959 CRU climate forcing) of Denali National Park and Preserve, Alaska. The values shown in shades of green, blue, and purple are active-layer thickness (ALT). The values shown in shades of brown and red are seasonally-frozen-layer thickness (SFLT). The ALT and SFLT map is draped over a hillshade model shown in grayscale. The hillshade model is apparent in places where snow-ice landcover class is masked out.

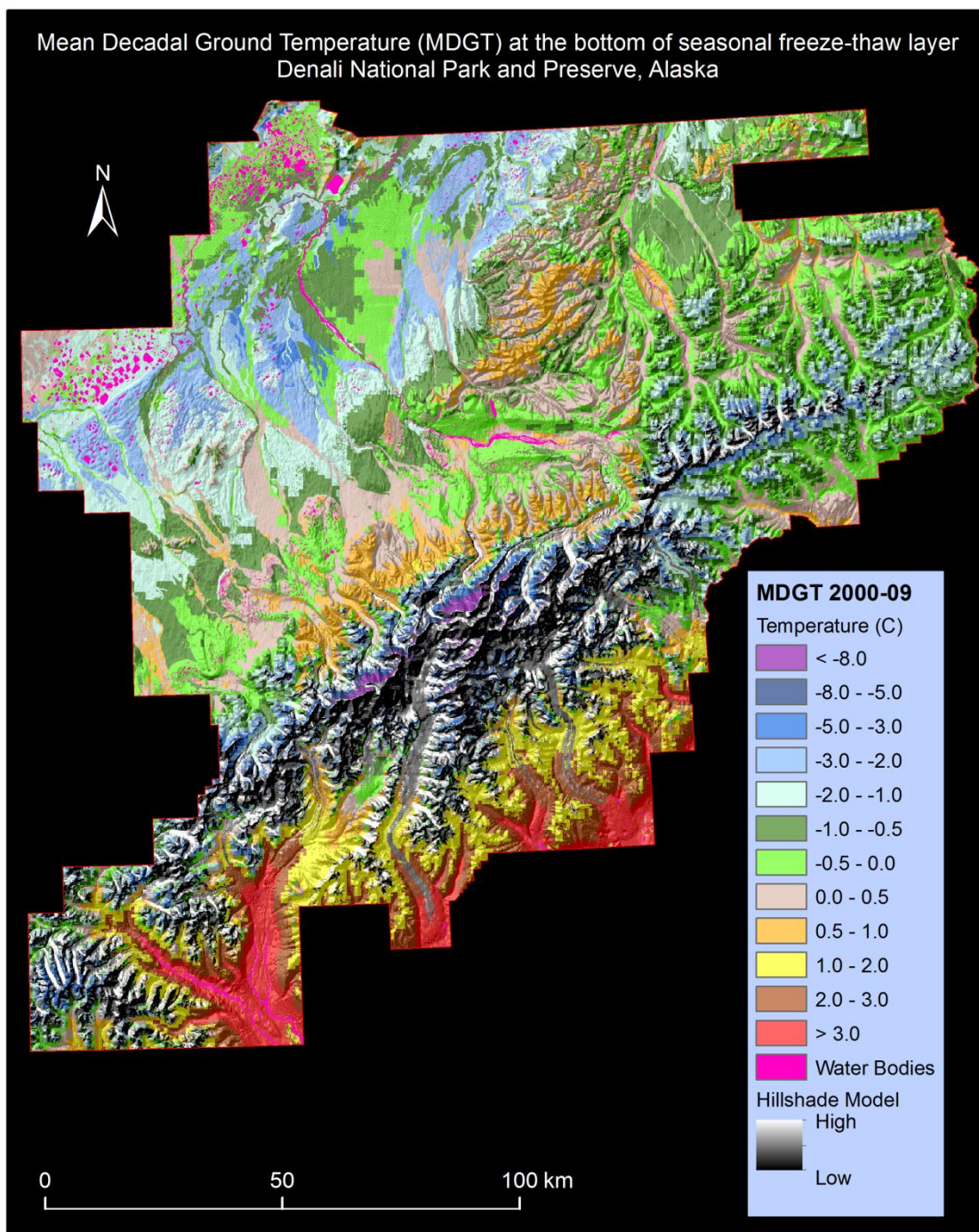


**Figure 5.** Permafrost map (2000-2009 CRU climate forcing) of Denali National Park and Preserve, Alaska. The negative temperature values, shown in shades of green and blue, indicate presence of near-surface permafrost. The positive temperature values, shown in shades of brown and red, indicate absence of near-surface permafrost. The acronym MDGT stands for Mean Decadal Ground Temperature. The MDGT map is draped over a hillshade model shown in grayscale. The hillshade model is apparent in places where snow-ice landcover class is masked out.

Active-Layer Thickness (ALT) & Seasonally-Frozen-Layer (SFLT) Thickness Map  
Denali National Park and Preserve, Alaska

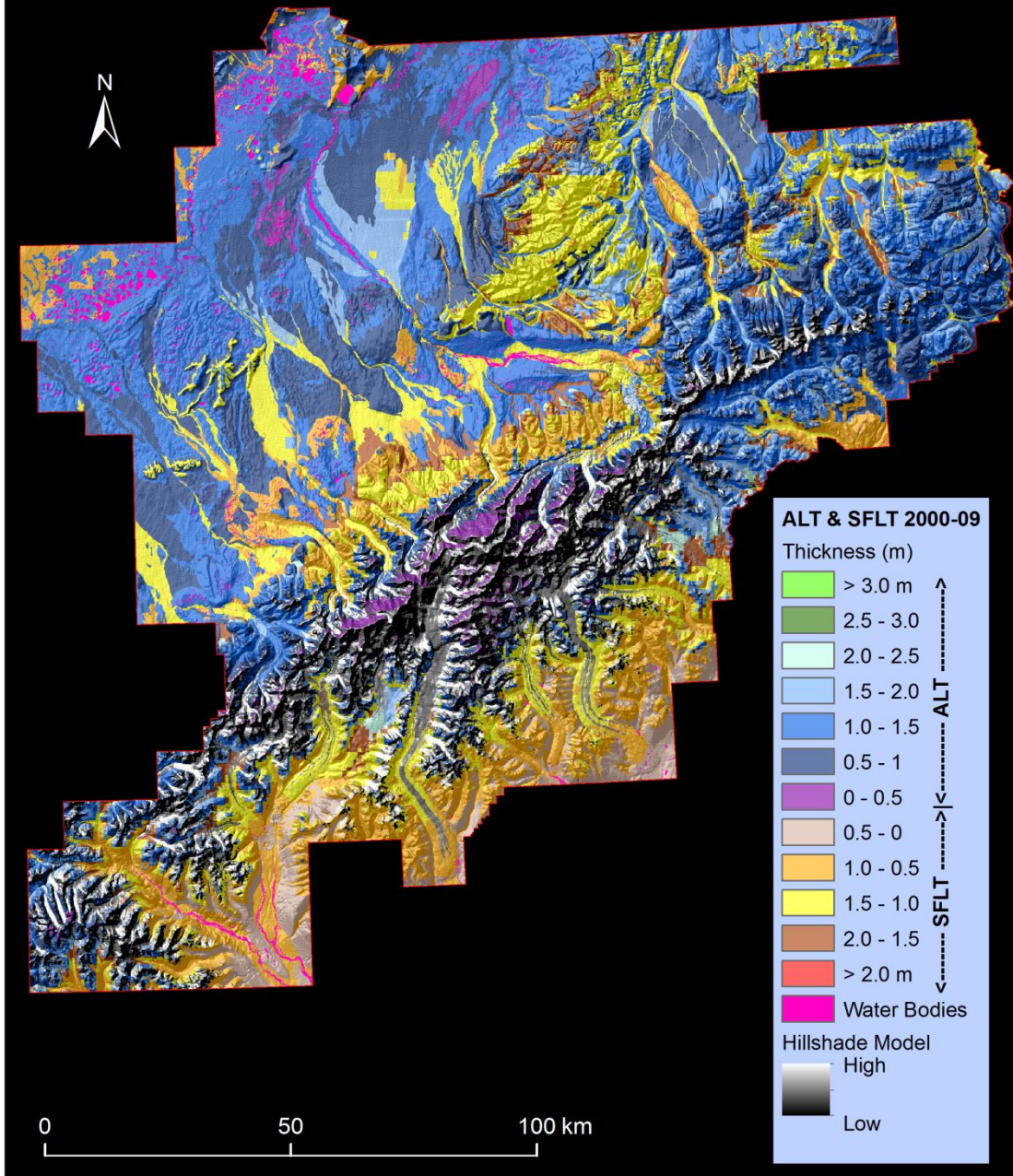


**Figure 6.** Active-layer and seasonally-frozen-layer thickness map (2000-2009 CRU climate forcing) of Denali National Park and Preserve, Alaska. The values shown in shades of green, blue, and purple are active-layer thickness (ALT). The values shown in shades of brown and red are seasonally-frozen-layer thickness (SFLT). The ALT and SFLT map is draped over a hillshade model shown in grayscale. The hillshade model is apparent in places where snow-ice landcover class is masked out.

**Table 1.** Summary statistics of climate and modeled permafrost characteristics in Denali National Park and Preserve using CRU climate forcing.

| <b>Climate characteristics</b>               | <b>1950-1959</b> | <b>2000-2009</b> |
|--|------------------|------------------|
| Decadal air temperature range (°C)           | -31.2 to 1.3     | -29.3 to 3.1     |
| Mean decadal air temperature (°C)            | -3.5             | -1.6             |
| Decadal precipitation range (mm)             | 304 to 2182      | 304 to 2090      |
| Mean decadal precipitation (mm)              | 679              | 651              |
| <b>Modeled permafrost characteristics</b>    |                  |                  |
| Mean decadal permafrost temperature (°C)     | -2.1             | -1.1             |
| Permafrost distribution (% of DENA area)     | 75               | 51               |
| Permafrost warmer than -1°C (% of DENA area) | 8.5              | 30               |
| Decadal ALT range (m)                        | 0.22 to 2.45     | 0.17 to 2.56     |
| Mean decadal ALT (m)                         | 1.1              | 1.1              |
| Decadal SFLT range (m)                       | 0.42 to 2.11     | 0.22 to 2.1      |
| Mean decadal SFLT (m)                        | 0.97             | 1.0              |
| ALT shallower than 1 m (% of DENA area)      | 38               | 19               |

## 5.2. 5-GCM Composite Climate Forcing (2001-2010, 2051-2060, and 2091-2100)

The bias-corrected 5-GCM composite decadal (2001-2010) air temperature and uncorrected precipitation resulted in a slight decrease in permafrost area as compared to the model permafrost distribution using CRU (2000-2009) climate forcing due to higher precipitation in (2001-2010) 5-GCM composite. In order to understand the future permafrost distribution and changes to its characteristics due to the projected climate warming, the modeling results from 5-GCM composite climate forcing should be compared and analyzed (Table 2).

The bias-corrected 5-GCM composite decadal (2001-2010) air temperature ranged from - 29.3 to 3.1°C and the mean was - 1.6°C. The decadal precipitation ranged from 332 to 2368 mm and the mean was 731 mm. The model mapped 49% of DENA total area as underlain by near-surface permafrost and the mean permafrost temperature was - 1.1°C, i.e., the majority of near-surface permafrost in DENA are warm permafrost and within a degree of freezing (Figure 7 and 8). The bias-corrected 5-GCM composite decadal air temperature suggests ~1.0°C increase in mean decadal air temperature by 2050s, consequently, the model predicts dramatic degradation of near-surface permafrost by 2050s. A mere 6% of DENA total area is predicted to have ‘stable’ near-surface permafrost by 2050s and 4% of the DENA total area is predicted to be underlain by permafrost within a degree of freezing (Figure 9 and 10, Table 2). The climate will continue to warm and the 5-GCM composite suggests another ~3.4°C increase in mean decadal air temperature by 2090s, i.e., a total of ~4.4°C increase in the air temperature between 2000s and 2090s. This is expected to cause further increase in ground temperature and degradation of near-surface permafrost. Only 1% of DENA total area is predicted to be underlain by ‘stable’ near-surface permafrost by the end of the 21<sup>st</sup> century (Figure 11 and 12), mostly on the north-facing slopes of high mountains. The near-surface permafrost, within the top 3 m of the ground surface, is predicted to be extinct from DENA by the end of the century.

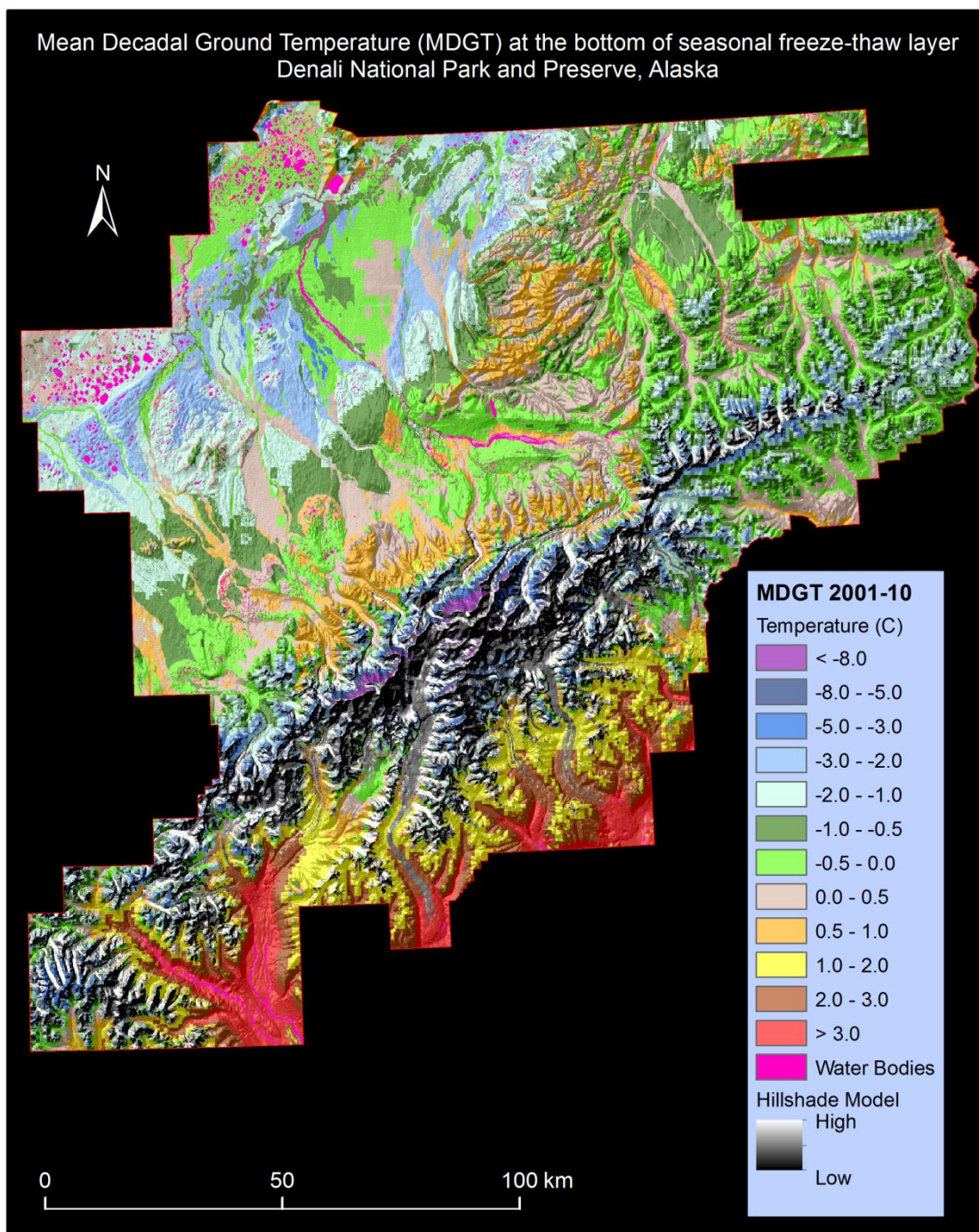


**Figure 7.** Permafrost map (2001-2010 5-GCM climate forcing) of Denali National Park and Preserve, Alaska. The negative temperature values, shown in shades of green and blue, indicate presence of near-surface permafrost. The positive temperature values, shown in shades of brown and red, indicate absence of near-surface permafrost. The acronym MDGT stands for Mean Decadal Ground Temperature. The MDGT map is draped over a hillshade model shown in grayscale. The hillshade model is apparent in places where snow-ice landcover class is masked out.

Active-Layer Thickness (ALT) & Seasonally-Frozen-Layer (SFLT) Thickness Map  
Denali National Park and Preserve, Alaska

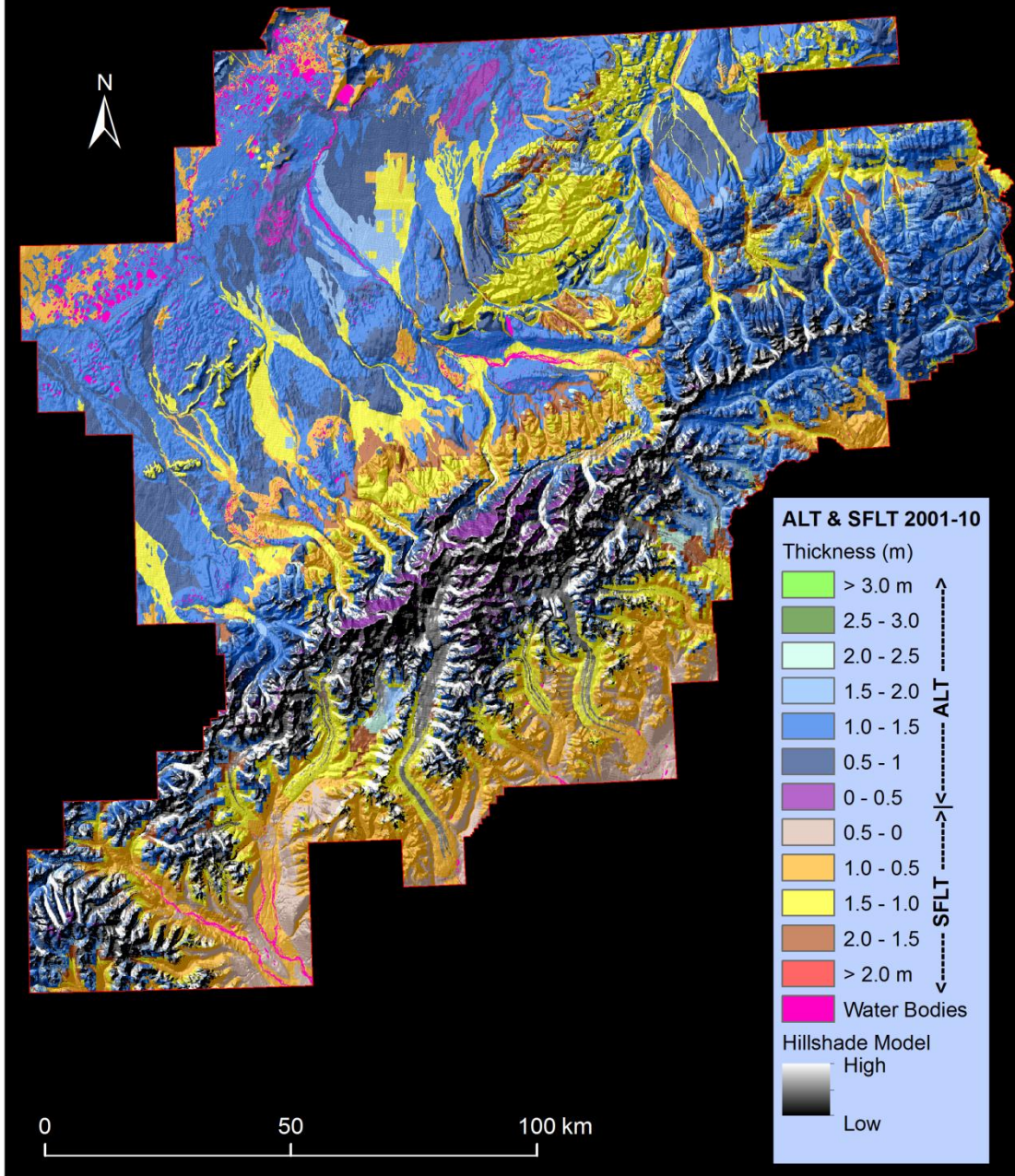


**Figure 8.** Active-layer and seasonally-frozen-layer thickness map (2001-2010 5-GCM climate forcing) of Denali National Park and Preserve, Alaska. The values shown in shades of green and purple are active-layer thickness (ALT). The values shown in shades of yellow and red are seasonally-frozen-layer thickness (SFLT). The ALT and SFLT map is draped over a hillshade model shown in grayscale. The hillshade model is apparent in places where snow-ice landcover class is masked out from the ALT and SFLT map.

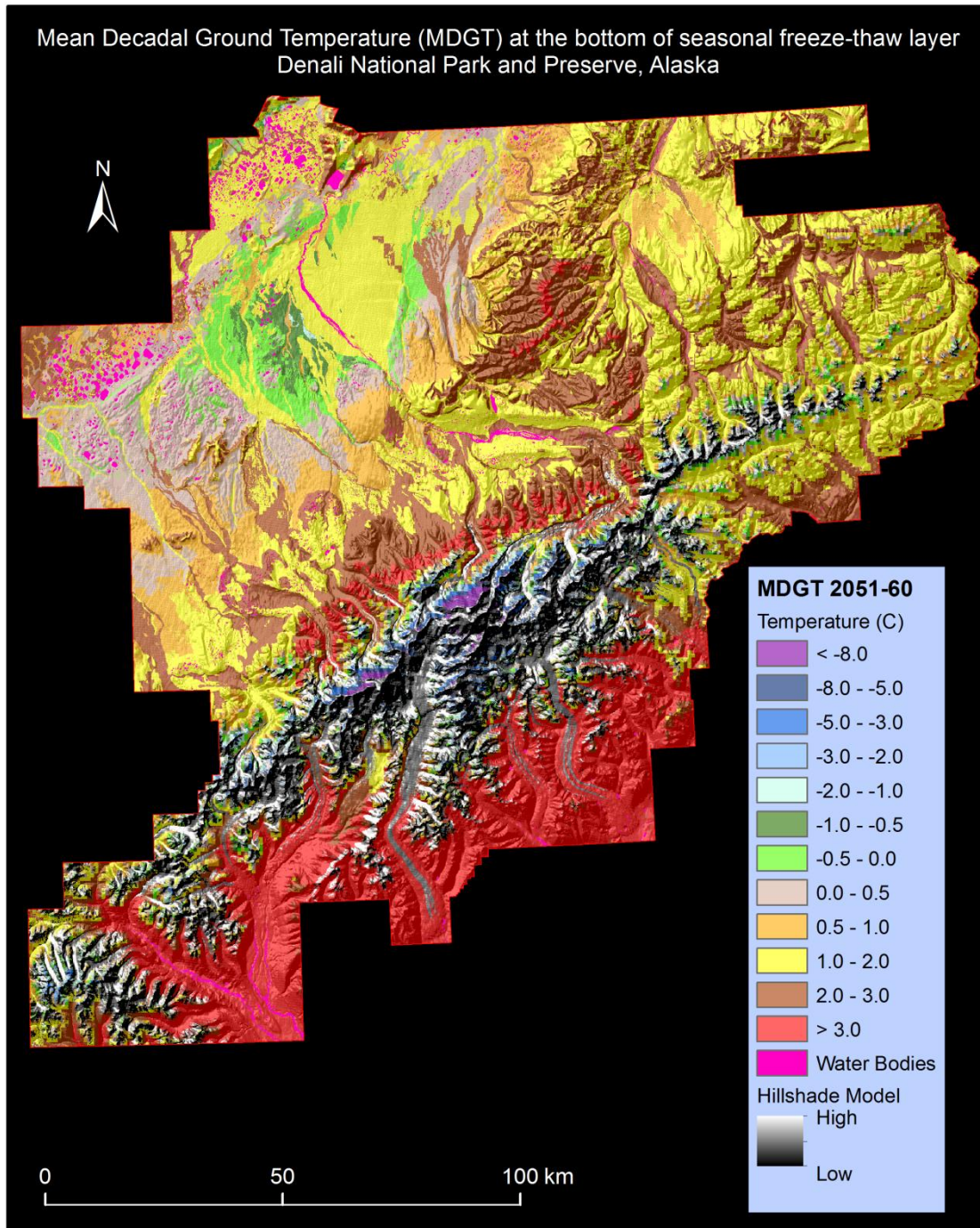


**Figure 9.** Permafrost map (2051-2060 5-GCM climate forcing) of Denali National Park and Preserve, Alaska. The negative temperature values, shown in shades of green and blue, indicate presence of near-surface permafrost. The positive temperature values, shown in shades of brown and red, indicate absence of near-surface permafrost. The acronym MDGT stands for Mean Decadal Ground Temperature. The MDGT map is draped over a hillshade model shown in grayscale. The hillshade model is apparent in places where snow-ice landcover class is masked out.

Active-Layer Thickness (ALT) & Seasonally-Frozen-Layer (SFLT) Thickness Map  
Denali National Park and Preserve, Alaska

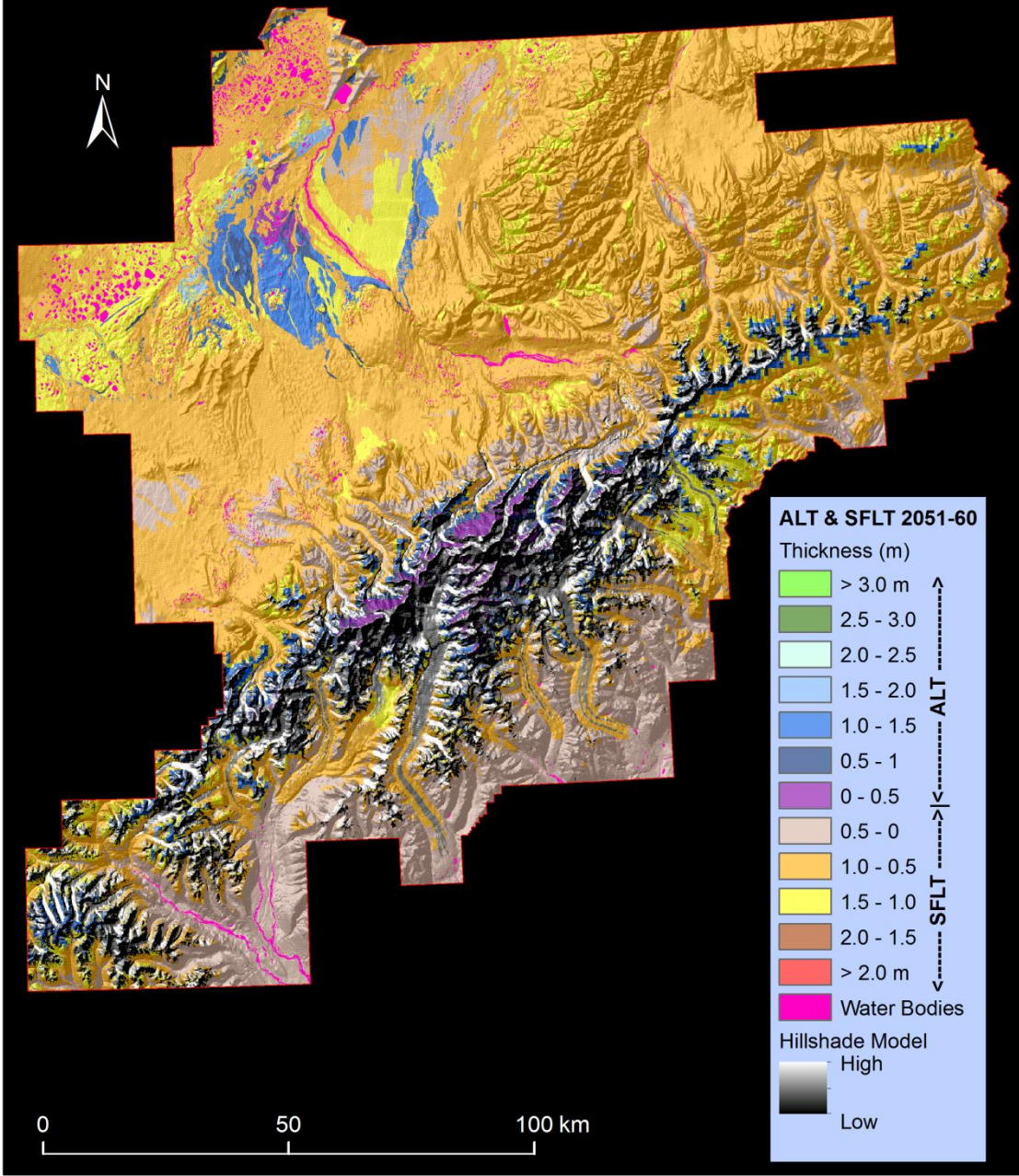


**Figure 10.** Active-layer and seasonally-frozen-layer thickness map (2051-2060 5-GCM climate forcing) of Denali National Park and Preserve, Alaska. The values shown in shades of green, blue, and purple are active-layer thickness (ALT). The values shown in shades of brown and red are seasonally-frozen-layer thickness (SFLT). The ALT and SFLT map is draped over a hillshade model shown in grayscale. The hill shade model is apparent in places where snow-ice landcover class is masked out.

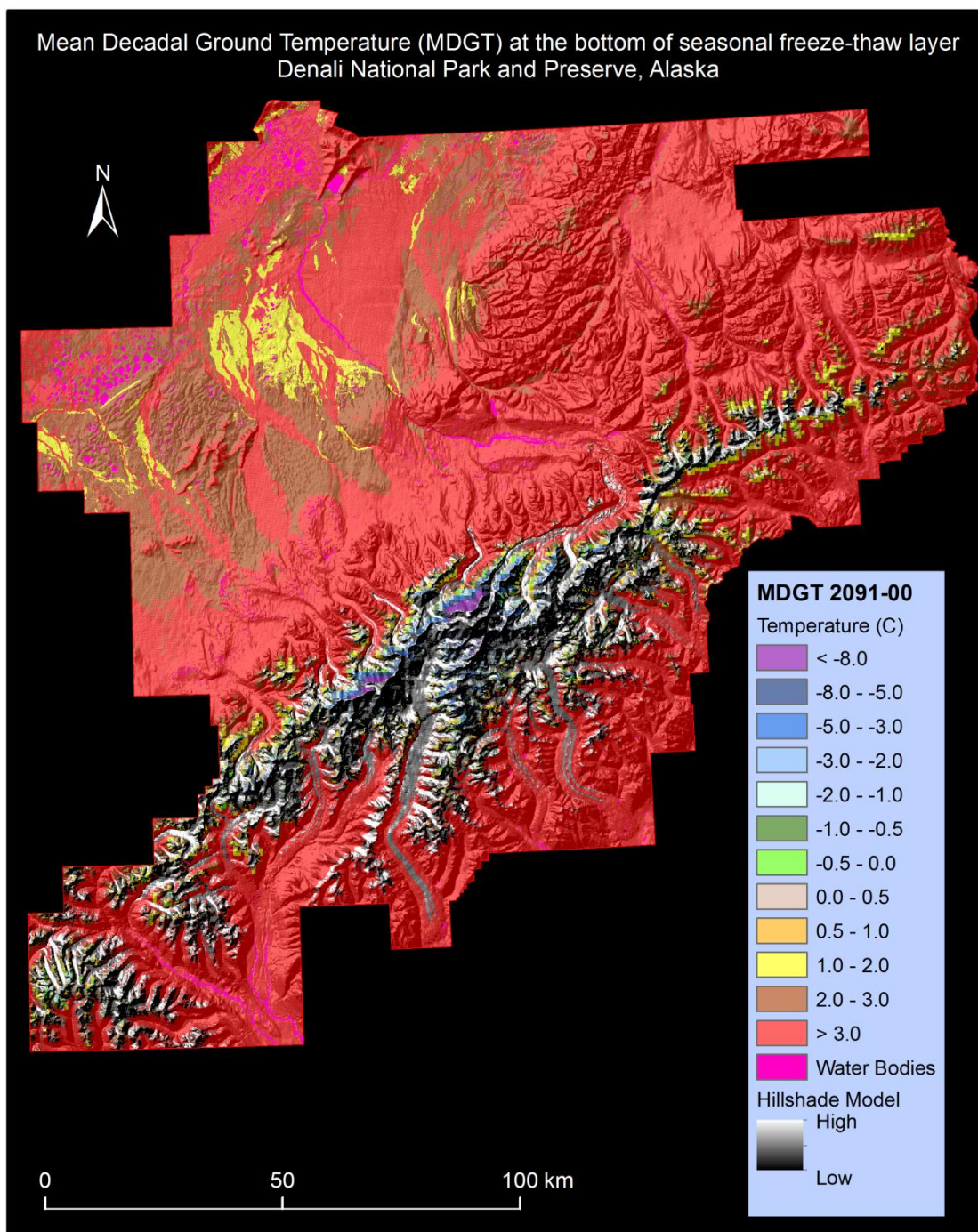


**Figure 11.** Permafrost map (2091-2100 5-GCM climate forcing) of Denali National Park and Preserve, Alaska. The negative temperature values, shown in shades of green and blue, indicate presence of near-surface permafrost. The positive temperature values, shown in shades of brown and red, indicate absence of near-surface permafrost. The acronym MDGT stands for Mean Decadal Ground Temperature. The MDGT map is draped over a hillshade model shown in grayscale. The hillshade model is apparent in places where snow-ice landcover class is masked out.

Active-Layer Thickness (ALT) & Seasonally-Frozen-Layer (SFLT) Thickness Map  
Denali National Park and Preserve, Alaska

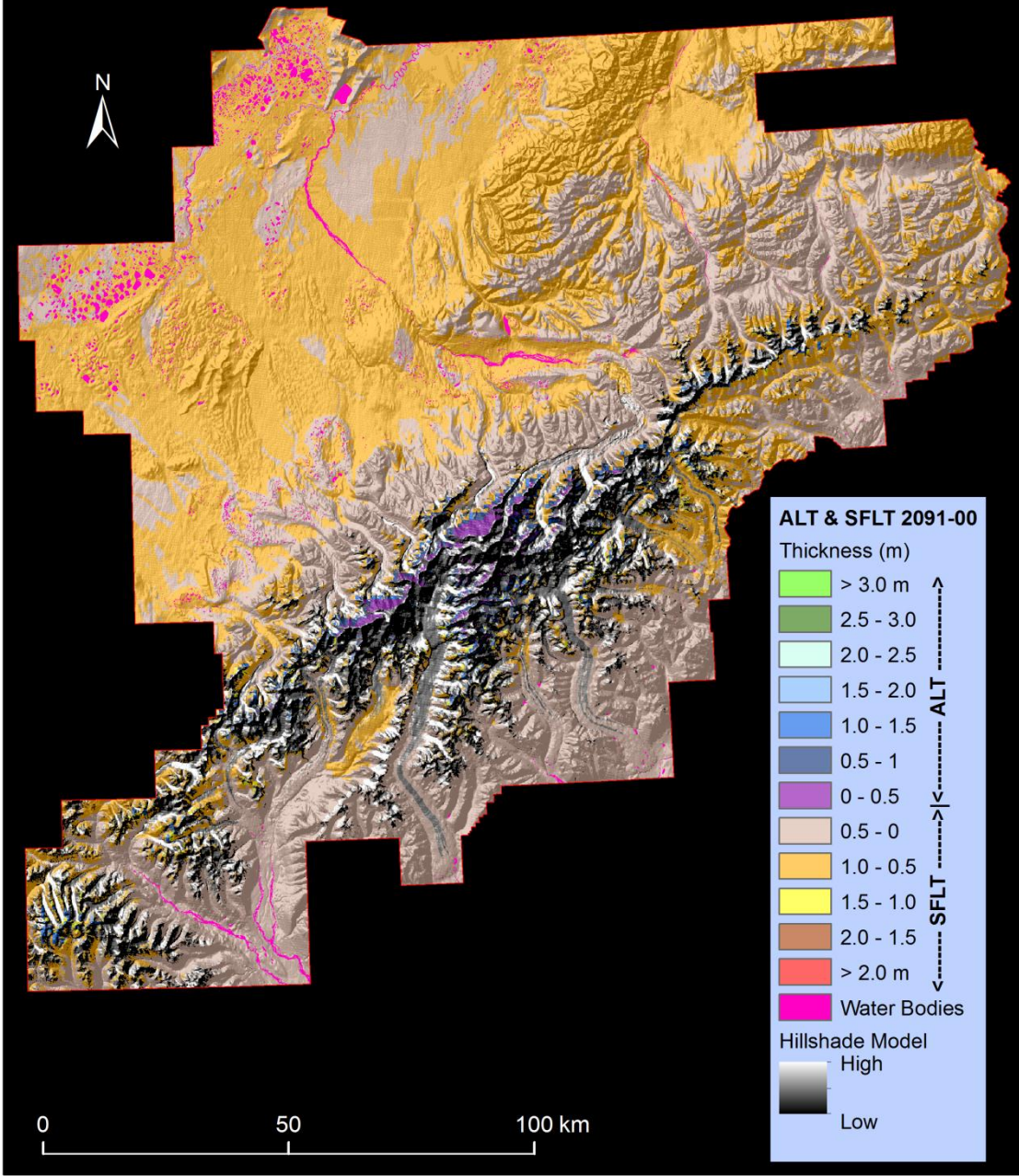


**Figure 12.** Active-layer and seasonally-frozen-layer thickness map (2091-2100 5-GCM climate forcing) of Denali National Park and Preserve, Alaska. The values shown in shades of green, blue, and purple are active-layer thickness (ALT). The values shown in shades of brown and red are seasonally-frozen-layer thickness (SFLT). The ALT and SFLT map is draped over a hillshade model shown in grayscale. The hillshade model is apparent in places where snow-ice landcover class is masked out.

**Table 2.** Summary statistics of climate and modeled permafrost characteristics in Denali National Park and Preserve using 5-GCM composite climate forcing.

| <b>Climate characteristics</b>               | <b>2001-2010</b> | <b>2051-2060</b> | <b>2091-2100</b> |
|--|------------------|------------------|------------------|
| Decadal air temperature range (°C)           | -29.3 to 3.1     | -27.0 to 5.3     | -25.0 to 7.3     |
| Mean decadal air temperature (°C)            | -1.6             | -0.7             | +2.7             |
| Decadal precipitation range (mm)             | 332 to 2368      | 380 to 2736      | 418 to 3061      |
| Mean precipitation (mm)                      | 731              | 845              | 938              |
| <b>Modeled permafrost characteristics</b>    |                  |                  |                  |
| Mean decadal permafrost temperature (°C)     | -1.1             | -1.3             | -3.3             |
| Permafrost distribution (% of DENA area)     | 49               | 6                | 1                |
| Permafrost warmer than -1°C (% of DENA area) | 30               | 4                | 0.3              |
| Decadal ALT range (m)                        | 0.18 to 2.57     | 0.21 to 1.79     | 0.22 to 1.60     |
| Mean decadal ALT (m)                         | 1.1              | 1.07             | 0.77             |
| Decadal SFLT range (m)                       | 0.22 to 2.18     | 0.13 to 1.50     | 0.03 to 1.35     |
| Mean decadal SFLT (m)                        | 1.0              | 0.72             | 0.48             |
| ALT shallower than 1 m (% of DENA area)      | 17               | 2                | 0.7              |

### 5.3. Accuracy Assessment

In order to assess the accuracy of the modeling products we performed two types of tests, warm-biased test and cold-biased test. The warm-biased test assesses if the modeled ground temperature is warm-biased i.e., warmer than the actual ground temperature and therefore mapped lesser permafrost extent within DENA. The cold-biased test assesses if the modeled ground temperature is cold-biased i.e., colder than the actual ground temperature and therefore mapped greater permafrost extent within DENA.

#### 5.3.1. Warm-biased Test

Clark and Duffy (2006) identified presence/absence of permafrost at 1615 field sites within DENA. They found permafrost at 648 sites, 408 of these sites were sampled in the latter part of the summer (i.e., August and September). We compared the 2000-2009 modeled permafrost map with the field-identified permafrost sites. We used the 408 sites sampled in August and September for this comparison and excluded the sites that were sampled before the month of August as those could be seasonally-frozen sites. At 49 of these late-summer-field-identified permafrost sites, the model predicted absence of near-surface permafrost. At the remaining 359 permafrost sites the model predicted the presence of near-surface permafrost in agreement with the field observations i.e., 88% agreement between 2000-2009 modeled permafrost map and field observations that were carried out during 1997-2002. The 49 sites where the model failed are confined to the northwest quadrant of DENA within Yukon-Kuskokwim Bottomlands and some parts of Alaska Mountain eco-sections. These findings suggest that the modeled permafrost maps may be slightly warm-biased at some sites in the northwest quadrant of DENA and thus could be mapping lesser permafrost extent there.

### **5.3.2. Cold-biased Test**

To test for the cold-bias we compared the permafrost-absent sites identified in the field with modeled permafrost temperature and active-layer or seasonally-frozen-layer thickness at those sites. The field crew inferred the lower depth of the last soil layer they sampled and the maximum sampling depth is not reported. So, we used the last soil layer upper depth and added 0.1 m to it assuming the field crew must have dug 0.1 m further into the last soil layer and used that value as the maximum depth of investigation.

Clark and Duffy (2006) did not find permafrost at 967 sites. We compared the 2000-2009 modeled permafrost map with the field identified permafrost-absent sites. At 743 sites out of the 967 permafrost-absent sites the model predicted presence of near-surface permafrost. By comparing the model predicted ALT at those 743 sites with the maximum depth of investigation, we found that at 590 sites the modeled ALT is deeper than the maximum depth of investigation which implies the field crew did not investigate deep enough to confirm the presence of permafrost. At the remaining 153 sites the model predicted ALT was shallower than the maximum depth of investigation i.e., at these sites the model falsely predicted presence of permafrost and hence in disagreement with field observations. So out of the 967 permafrost-absent sites, the modeled (2000-2009) permafrost map is in agreement with field observations at 814 sites or 84% agreement. The 153 sites where the model failed are scattered throughout the Yukon-Kuskokwim Bottomlands and Alaska Mountain eco-sections. Our model mapped continuous permafrost in the floodplains of McKinley River and Slippery Creek which likely underlain by discontinuous or sporadic permafrost (Adema 2006). This is because GIPL 1.0 models heat transfer through conduction and does not account for the heat transfer through convection which may be the dominant mechanism of heat transfer in the floodplain due to the movement of surface and subsurface water. The test suggests that the modeling products may be slightly cold-biased at some sites within Yukon-Kuskokwim Bottomlands and Alaska Mountain eco-sections and thus could be mapping greater permafrost extent at those sites.

The warm-biased and cold-biased tests used 408 and 967 field observations within DENA, respectively, to determine the accuracy of the modeling products. The two tests together resulted in 86% agreement between field-observed and modeled permafrost presence/ absence within DENA. Hence, we conclude that the modeled permafrost temperature and active-layer thickness maps are reliable representation of near-surface permafrost distribution within DENA. However, we do not rule out the presence of permafrost at a deeper depth where the model did not map near-surface permafrost because GIPL 1.0 is an equilibrium model (Appendix B) and predicts presence or absence of near-surface permafrost only at the bottom of seasonal freeze-thaw layer.

### **5.3.3. Comparison with Recorded Ground Temperature**

At three climate-monitoring stations within DENA the NPS began collecting ground temperature data since 2005; the three stations are Dunkle Hills, Stampede, and Toklat (<http://www.wrcc.dri.edu/denali/>). We summarized the available ground temperature data from these stations and compared them with the modeled ground temperatures (Table 3).

The average (2005-2010) air temperature at these climate stations are 1-2.5°C colder than the CRU decadal air temperature. We attribute this temperature difference to the difference in scale of the two

datasets. The climate station temperature records are from a single location whereas CRU temperatures are spatially averaged temperature from a global climate datasets of  $0.5^\circ \times 0.5^\circ$  latitude-longitude resolution, downscaled to 771 m by SNAP. SNAP utilized PRISM (Parameter-elevation Regressions on Independent Slope Model) spatial climate data at 771 m spatial resolution for downscaling. The PRISM data are developed with a statistical model that accounts for land features such as slope, elevation and coastlines. So the PRISM data assigns a single slope and elevation value to a 771 m cell, but in reality both slope and elevation can vary substantially within a 771 m cell especially in areas of high relief. The three concerned climate stations are located in areas of high relief (Figure 13). Thus the difference in local topography, which strongly influences near-surface air temperature, between the climate stations and 771 m PRISM data cells is majorly responsible for the temperature difference between them. A detail description of the SNAP downscaling procedure can be found here (<http://www.snap.uaf.edu/downscaling.php>). We further downscaled the CRU air temperature data by dividing its 771 m cells to 28 m cells to be compatible with the soil and ecotype inputs for high-resolution modeling. The difference in the averaging periods, 5-year of climate stations record vs. 10-year of CRU data, may also be contributing to the temperature difference between the climate stations and the CRU data.

The modeled ground surface temperatures are  $0.8^\circ\text{C}$  and  $0.5^\circ\text{C}$  colder, and  $0.5^\circ\text{C}$  warmer than the recorded ground temperature (at 0.02 m) at Dunkle Hills, Toklat, and Stampede climate stations, respectively. Since the GIPL 1.0 model uses a homogeneous layer approach to account for the insulating effects of snow, surface organic, and seasonal freeze-thaw layers the smaller difference between modeled ground surface temperatures and recorded near-surface ground temperatures at the climate stations exude confidence on the ability of the model to predict temperature at the bottom seasonal freeze-thaw layer. However, it also shows that to some degree the model underestimates the insulating effect of snow as the modeled insulating effect of snow ranges from  $2 - 2.5^\circ\text{C}$  whereas the recorded temperatures show  $\sim 4.0^\circ\text{C}$  difference between near-surface air and ground temperatures. This difference can be attributed to three major factors: 1) scale, 2) ground condition, and 3) snow depth. 1) We compared the ground temperature recorded at a single location with modeled (average) ground temperature that used climate input derived from a global climate dataset of  $0.5^\circ \times 0.5^\circ$  latitude-longitude resolution. 2) The difference in ground condition, type and thickness of surface organic layer and seasonal moisture variation, between what really exists at the climate station vs. the generalized ecotype used as the model input. 3) The snow depth at the climate station could be significantly different than the snow depth estimated by the model because the model uses a simple linear approach to convert the winter precipitation to snow depth by assuming a fixed density of the snow which depends on the type of snow at that location. The snow algorithm does not model the effect of wind on snow distribution. Also, both precipitation input and snow classes are derived from km scale datasets. So the true snow depth and density at a point location can be significantly different than what used as the model input for that location.

**Table 3.** Comparison of recorded air and ground temperatures at the NPS climate stations with CRU air temperature and modeled temperature at the ground surface and bottom of seasonal freeze-thaw layer. The temperature averaging periods are in parentheses (Note: we summarized ground temperature data only for years that have  $\geq 350$  days of data).

| <b>Recorded</b>  | <b>Dunkle Hills</b><br>Lat: 63.27 °N<br>Lon: 149.54 °W | <b>Stampede</b><br>Lat: 63.75 °N<br>Lon: 150.33 °W | <b>Toklat</b><br>Lat: 63.52 °N<br>Lon: 150.04 °W |
|--|--|--|--|
| Average air temperature  | -2.8°C<br>(2005-2010)                                  | -4.1°C<br>(2005-2010)                              | -3.1°C<br>(2006-2010)                            |
| Average ground temperature at 0.02 m   | 1.1°C<br>(2005-2010)                                   | 0.4°C<br>(2005-2010)                               | 1.0°C<br>(2006-2010)                             |
| Average ground temperature at 0.1 m  | 0.8°C<br>(2006-2010)                                   | 1.0°C<br>(2008-2010)                               | 1.4°C<br>(2006-2010)                             |
| <b>Projected</b>   |  |  |  |
| CRU average air temperature (2000-2009)  | -1.8°C   | -1.6°C   | -1.4°C   |
| <b>Modeled</b>   |  |  |  |
| Average ground surface temperature (2000-2009)                                     | 0.3°C  | 0.9°C  | 0.56°C   |
| Average ground temperature at the bottom of seasonal freeze-thaw layer (2000-2009) | 0.1°C at 0.75 m  | -0.6°C at 1.12m                                    | 0.1°C at 1.0 m                                   |

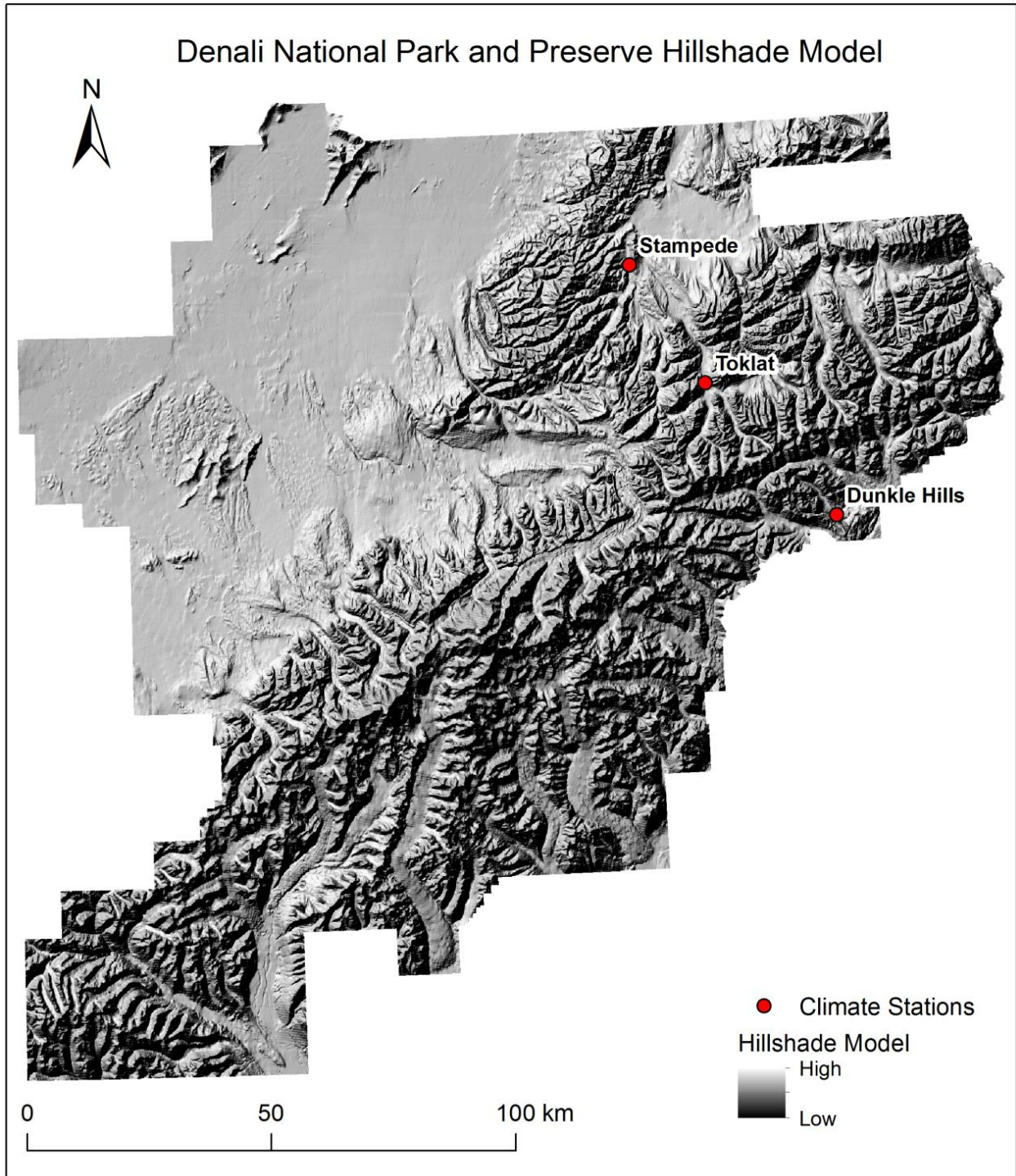


**Figure 13.** Locations of three climate stations plotted on a Denali National Park and Preserve Hillshade Model. The Hillshade Model is derived from 2-arc-second (~60 m) spatial resolution National Elevation Dataset Digital Elevation Model.

## 6. Deliverables

Deliverables for this project include the following raster (.tif and .png) and legend (.lyr) data files:

- Mean decadal ground temperature, at the bottom of seasonal freeze-thaw layer, raster (DENA-MDGT-####-##.tif) layers of Denali National Park and Preserve for the time periods 1950-1959, 2000-2009, 2001-2010, 2051-2060, and 2091-2100.
- Mean decadal ground temperature legend (DENA-MDGT-Legend.lyr) file.
- Mean decadal ground temperature, at the top of permafrost or bottom of seasonally-frozen layer, maps (DENA-MDGT-####-##.png) for the time periods 1950-1959, 2000-2009, 2001-2010, 2051-2060, and 2091-2100.
- Active-layer and seasonally-frozen-layer thickness raster layers (DENA-ALT-SFLT-####-##.tif) of Denali National Park and Preserve for the time periods 1950-1959, 2000-2009, 2001-2010, 2051-2060, and 2091-2100.
- Active-layer and seasonally-frozen-layer thickness legend (DENA-ALT-SFLT-Legend.lyr) file.
- Active-layer and seasonally-frozen-layer maps (DENA-ALT-SFLT-####-##.png) for the time periods 1950-1959, 2000-2009, 2001-2010, 2051-2060, and 2091-2100.

## 7. Literature Cited

- Adema, G. 2006. Permafrost landscapes. Unpublished report. National Park Service, Denali National Park and Preserve, Denali Park, AK.
- Brown, J., O. J. Ferrians, Jr., J. A. Heginbottom, and E. S. Melnikov. 1997. Circum-Arctic map of permafrost and ground ice conditions. CP-45. US Geological Survey, Reston, VA.
- Burn, C. R. 1998. The active layer: Two contrasting definitions. *Permafrost and Periglacial Processes* 9:411–416.
- Clark, M. H., and M. S. Duffy. 2006. Soil survey of Denali National Park area, Alaska. National Cooperative Soil Survey, 822 p.
- ECOMAP. 1993. National hierarchical framework of ecological units. United States Department of Agriculture, US Forest Service, Washington, D.C.
- Ferrians, O. J., Jr. 1965. Permafrost map of Alaska. United States Geological Survey Miscellaneous Investigation, Map I-445, scale 1:2,500,000.
- French, H., and Y. Shur. 2010. The principles of cryostratigraphy. *Earth-Science Reviews* 101:190–206.
- Jorgenson, M. T., and T. E. Osterkamp. 2005. Response of boreal ecosystems to varying modes of permafrost degradation. *Canadian Journal of Forest Research* 35:2100–2111.
- Jorgenson, M. T., C. H. Racine, J. C. Walters, and T. E. Osterkamp. 2001. Permafrost degradation and ecological changes associated with a warming climate in central Alaska. *Climate Change* 48:551–579.
- Jorgenson, M. T., K. Yoshikawa, M. Kanevskiy, and Y. Shur. 2008. Permafrost characteristics of Alaska. Institute of Northern Engineering, University of Alaska Fairbanks, 1 Sheet, Scale 1: 7,200,000.
- Kanevskiy, M., Y. Shur, D. Fortier, M. T. Jorgenson, and E. Stephani. 2011. Cryostratigraphy of late Pleistocene syngenetic permafrost (yedoma) in northern Alaska, Itkillik River exposure. *Quaternary Research* 75(3):584–596.
- Lachenbruch, A. H. 1959. Periodic heat flow in a stratified medium with application to permafrost problems. *US Geological Survey Bulletin*, 1083-A, 36 p.
- Lawler, J. P., S. D. Miller, D. M. Sanzone, J. Ver Hoef, and S. B. Young. 2009. Arctic network vital signs monitoring plan. Natural Resource Report NPS/ARC/NRR—2009/088. U.S. Department of the Interior, National Park Service, Natural Resource Program Center, Ft. Collins, CO.

- Loveland, T. R., Z. Zhu, D. O. Ohlen, J. F. Brown, B. C. Reed, L. Yang. 1999. An analysis of the IGBP global land-cover characterization process. *Photogrammetric Engineering and Remote Sensing* 65(9):1021–32.
- MacCluskie, M., and K. Oakley. 2005. Vital signs monitoring plan, Central Alaska Network. August 2005. U.S. Department of the Interior, National Park Service, Fairbanks, AK.
- Marchenko, S., V. Romanovsky, and G. Tipenko. 2008. Numerical modeling of spatial permafrost dynamics in Alaska. In the Proceedings of Ninth International Conference on Permafrost, June 2008, Vol. 2: 1125–30.
- Muller, S. W. 1947. Permafrost or permanently frozen ground and related engineering problems. W. Edwards, Inc., Ann Arbor, MI. 231 p.
- Nowacki, G., and T. Brock. 1995. Alaska-Ecomap version 2.0. United States Department of Agriculture, U.S. Forest Service. Available from <http://agdc.usgs.gov/data/usgs/erosafo/ecoreg/index.html> (accessed March 2014).
- Osterkamp, T. E. 2007. Characteristics of the recent warming of permafrost in Alaska. *Journal of Geophysical Research* 112:F02S02, doi:10.1029/2006JF000578.
- Osterkamp, T. E., and M. T. Jorgenson. 2009. Permafrost conditions and processes. Pages 205–227 *in* R. Young and L. Norby, editors. *Geological monitoring*: Boulder, Colorado, Geological Society of America.
- Osterkamp, T. E., M. T. Jorgenson, E. A. G. Schuur, Y. L. Shur, M. Z. Kanevskiy, J. G. Vogel and V. E. Tumskoy. 2009. Physical and ecological changes associated with warming permafrost and thermokarst in Interior Alaska. *Permafrost and Periglacial Processes* 20:235–256.
- Romanovsky, V. E. 1987. Approximate calculation of the insulation effect of the snow cover. *Geokriologicheskie Issledovania* (in Russian), MGU Press 23:145–157.
- Romanovsky, V. E., Y. Shur, K. Yoshikawa, and G. S. Tipenko. 2010a. Establishing a permafrost observatory at the Gakona HAARP site. Permafrost Laboratory. Available at <http://permafrost.gi.alaska.edu/project/establishing-permafrost-observatory-gakona-haarp-site> (accessed 17 May 2013).
- Romanovsky, V. E., S. L. Smith, and H. H. Christiansen. 2010b. Permafrost thermal state in the Polar Northern Hemisphere during the International Polar Year 2007–2009: a synthesis. *Permafrost and Periglacial Processes* 21:106–116.
- Sazonova, T. S., and V. E. Romanovsky. 2003. A model for regional-scale estimation of temporal and spatial variability of active-layer thickness and mean annual ground temperatures. *Permafrost and Periglacial Processes* 14:125–139.

- SNAP (Scenarios Network for Alaska and Arctic Planning). 2012. Tools and Data, Data. Available at <http://www.snap.uaf.edu/data.php> (accessed 27 January 2012).
- Schuur, E. A. G., J. Bockheim, J. G. Canadell, E. Euskirchen, C. B. Field, S. V. Goryachkin, S. Hagemann, P. Kuhry, P. M. Lafleur, H. Lee, and others. 2008. Vulnerability of permafrost carbon to climate change: Implications for the global carbon cycle. *BioScience* 58(8):701–714.
- Stevens, J. L., K. Boggs, A. Garibaldi, J. Grunblatt, and T. Helt. 2001. Denali National Park and Preserve landcover mapping project Volume 1: Remote sensing data, procedures and results. Natural Resource Technical Report NPS/DENA/NRTR—2001/001. National Park Service, Fort Collins, CO.
- Sturm, M., J. Holmgren, and G. E. Liston. 1995. A seasonal snow cover classification system for local to global applications. *Journal of Climate* 8(5):1261–1283.
- Van Everdingen, R. O. 1998. Multi-language glossary of permafrost and related ground ice terms. International Permafrost Association, National Snow and Ice Data Center, University of Colorado, Boulder.
- Viereck, L. A., C. T. Dyrness, A. R. Batten, and K. J. Wenzlick. 1992. The Alaska vegetation classification. General Technical Report, PNW-GTR-286. Pacific Northwest Research Station, U.S. Forest Service, Portland, OR.
- Walsh, J. E., W. L. Chapma, V. Romanovsky, J. H. Christensen, and M. Stendel. 2008. Global climate model performance over Alaska and Greenland. *American Meteorological Society* 21:6156–6174.
- Yershov, E. D. 1984. Thermal-physical properties of earth materials. Moscow State University Publication, p. 203 (In Russian).
- Yocum, L. C., G. W. Adema, and C. K. Hults. 2006. A baseline study of permafrost in the Toklat basin, Denali National Park and Preserve. Proceedings of the Central Alaska Park Science Symposium, September 12–14, 2006. Vol. 6(2):37–40.

## Appendix A. Tables of Landcover Classes, Landtype Associations, and Snow Classes

**Table A1.** Twenty out of the twenty five landcover classes mapped within DENA by Stevens et al. (2001) are used as ecotype input to the model. In the absence of thermal diffusivity data of surface organic layer for DENA ecotypes we prescribed these values based on our permafrost modeling experience in other parts of Alaska.

| Ecotype no. | Ecotype name                      | Thawed diffusivity (m <sup>2</sup> /s) | Frozen diffusivity (m <sup>2</sup> /s) | Thickness (m) |
|-------------|-----------------------------------|--|--|---------------|
| 1           | Dense open spruce                 | 1.47e <sup>-6</sup>                    | 2.50e <sup>-6</sup>                    | 0.10          |
| 2           | Open-woodland spruce              | 1.47e <sup>-6</sup>                    | 3.74e <sup>-6</sup>                    | 0.13          |
| 3           | Stunted spruce                    | 1.01e <sup>-6</sup>                    | 2.01e <sup>-6</sup>                    | 0.30          |
| 4           | Broadleaf                         | 1.01e <sup>-6</sup>                    | 2.01e <sup>-6</sup>                    | 0.10          |
| 5           | Spruce-broadleaf                  | 1.36e <sup>-6</sup>                    | 1.06e <sup>-6</sup>                    | 0.04          |
| 6           | Alder                             | 1.87e <sup>-6</sup>                    | 1.22e <sup>-6</sup>                    | 0.13          |
| 7           | Willow                            | 1.37e <sup>-6</sup>                    | 1.05e <sup>-6</sup>                    | 0.10          |
| 8           | Closed low birch shrub            | 1.47e <sup>-6</sup>                    | 1.02e <sup>-6</sup>                    | 0.07          |
| 9           | Low shrub birch/Ericaceous/Willow | 1.47e <sup>-6</sup>                    | 1.02e <sup>-6</sup>                    | 0.05          |
| 10          | Low shrub-sedge                   | 1.48e <sup>-6</sup>                    | 1.15e <sup>-6</sup>                    | 0.01          |
| 11          | Peatland                          | 1.05e <sup>-6</sup>                    | 1.95e <sup>-6</sup>                    | 0.50          |
| 12          | Herbaceous-shrub                  | 1.00e <sup>-6</sup>                    | 1.00e <sup>-6</sup>                    | 0.04          |
| 13          | Mixed dwarf shrub                 | 1.00e <sup>-6</sup>                    | 1.00e <sup>-6</sup>                    | 0.03          |
| 14          | Mixed dwarf shrub-rock            | 2.48e <sup>-6</sup>                    | 1.29e <sup>-6</sup>                    | 0.02          |
| 15          | Dry-mesic Herbaceous              | 1.18e <sup>-6</sup>                    | 1.12e <sup>-6</sup>                    | 0.15          |
| 16          | Wet Herbaceous                    | 1.58e <sup>-6</sup>                    | 1.16e <sup>-6</sup>                    | 0.09          |
| 17          | Aquatic Herbaceous                | 1.00e <sup>-6</sup>                    | 3.00e <sup>-6</sup>                    | 0.05          |
| 18          | Sparse Vegetation                 | 2.48e <sup>-6</sup>                    | 1.29e <sup>-6</sup>                    | 0.01          |
| 19          | Bare ground                       | 2.48e <sup>-6</sup>                    | 1.29e <sup>-6</sup>                    | 0.00          |
| 20          | Burn                              | 1.47e <sup>-6</sup>                    | 3.74e <sup>-6</sup>                    | 0.05          |

**Table A2.** One hundred-and-fifty-one out of 152 landtype associations identified within DENA by Clark and Duffy (2006) are used as soil type input to the model. The water landtype association is excluded from modeling. We referred to Yershov (1984) to prescribe the soil thermal properties.

| No. | Landtype association   | Thawed heat capacity (MJ/m <sup>3</sup> .K) | Frozen heat capacity (MJ/m <sup>3</sup> .K) | Thawed thermal conductivity (W/m.K) | Frozen thermal conductivity (W/m.K) | Volumetric water content (%) |
|-----|--|---|---|-------------------------------------|-------------------------------------|------------------------------|
| 1   | Boreal mica-rich low mountain foot slopes with continuous permafrost | 2.34  | 1.76  | 0.77                                | 1.12                                | 0.13                         |
| 2   | Boreal mica-rich low mountains                                       | 2.92  | 1.18  | 1.29                                | 1.21                                | 0.27                         |
| 3   | Boreal plateaus with continuous permafrost                           | 2.39  | 1.71  | 0.99                                | 1.45                                | 0.14                         |
| 4   | Boreal plains with discontinuous permafrost                          | 2.34  | 1.76  | 0.97                                | 1.09                                | 0.13                         |

| No. | Landtype association  | Thawed heat capacity (MJ/m <sup>3</sup> .K) | Frozen heat capacity (MJ/m <sup>3</sup> .K) | Thawed thermal conductivity (W/m.K) | Frozen thermal conductivity (W/m.K) | Volumetric water content (%) |
|-----|---|---|---|-------------------------------------|-------------------------------------|------------------------------|
| 5   | Boreal terraces with discontinuous permafrost                       | 2.40  | 1.70  | 0.91                                | 1.04                                | 0.14                         |
| 6   | Alpine schist mountain ridges with discontinuous permafrost         | 2.14  | 1.96  | 1.70                                | 1.86                                | 0.08                         |
| 7   | Alpine and subalpine schist mountain valleys                        | 2.14  | 1.96  | 1.70                                | 1.86                                | 0.08                         |
| 8   | Boreal eolian plains and dunes with discontinuous permafrost        | 2.42  | 1.68  | 0.81                                | 0.81                                | 0.15                         |
| 9   | Alpine and subalpine schist mountains                               | 2.14  | 1.96  | 1.95                                | 1.97                                | 0.08                         |
| 10  | Boreal groundwater discharge plains with discontinuous permafrost   | 2.70  | 1.40  | 0.90                                | 0.90                                | 0.21                         |
| 11  | Boreal Terrace escarpments with discontinuous permafrost            | 2.36  | 1.73  | 1.44                                | 1.52                                | 0.13                         |
| 12  | Alpine plains with continuous permafrost                            | 2.45  | 1.65  | 0.97                                | 1.43                                | 0.15                         |
| 13  | Boreal and subalpine schist mountains with discontinuous permafrost | 2.29  | 1.80  | 1.57                                | 1.78                                | 0.12                         |
| 14  | Boreal terraces with continuous permafrost, wet                     | 2.63  | 1.47  | 0.95                                | 1.34                                | 0.20                         |
| 15  | Boreal peat plateaus and loess plains with continuous permafrost    | 3.28  | 0.82  | 0.33                                | 0.44                                | 0.35                         |
| 16  | Boreal flood plains with discontinuous permafrost, Minchumina Basin | 2.65  | 1.45  | 1.00                                | 1.17                                | 0.20                         |
| 17  | Boreal plateaus with continuous permafrost, Wet                     | 2.45  | 1.65  | 0.97                                | 1.43                                | 0.15                         |
| 18  | Alpine schist mountain summits with discontinuous permafrost        | 2.28  | 1.81  | 1.12                                | 1.44                                | 0.11                         |
| 19  | Boreal terraces and high flood plains with discontinuous permafrost | 2.21  | 1.89  | 1.50                                | 1.71                                | 0.10                         |
| 20  | Boreal terraces with discontinuous permafrost, Minchumina basin     | 2.40  | 1.7   | 0.91                                | 1.04                                | 0.14                         |
| 21  | Boreal terraces with continuous permafrost, very wet                | 2.63  | 1.47  | 0.75                                | 1.27                                | 0.20                         |
| 22  | Boreal ice cored loess hills and plains with continuous permafrost  | 2.34  | 1.76  | 0.97                                | 1.40                                | 0.13                         |
| 23  | Boreal loess plains with continuous permafrost                      | 2.47  | 1.63  | 0.83                                | 1.31                                | 0.16                         |
| 24  | Boreal loess plains and hills with continuous permafrost            | 2.34  | 1.76  | 0.97                                | 1.39                                | 0.13                         |
| 25  | Boreal dissected plateaus with discontinuous permafrost             | 2.40  | 1.71  | 0.10                                | 1.45                                | 0.14                         |
| 26  | Boreal lower mountain slopes, Thermokarsted                         | 2.47  | 1.63  | 1.16                                | 1.62                                | 0.16                         |

| No. | Landtype association  | Thawed heat capacity (MJ/m <sup>3</sup> .K) | Frozen heat capacity (MJ/m <sup>3</sup> .K) | Thawed thermal conductivity (W/m.K) | Frozen thermal conductivity (W/m.K) | Volumetric water content (%) |
|-----|---|---|---|-------------------------------------|-------------------------------------|------------------------------|
| 27  | Boreal flood plains, High elevation   | 2.21  | 1.89  | 1.50                                | 1.71                                | 0.10                         |
| 28  | Boreal schist mountain backslopes with discontinuous permafrost                       | 2.23  | 1.87  | 1.52                                | 1.55                                | 0.10                         |
| 29  | Boreal terraces and plateau toeslopes with continuous permafrost                      | 2.47  | 1.63  | 0.90                                | 1.35                                | 0.16                         |
| 30  | Alpine low loess mountains with discontinuous permafrost                              | 2.43  | 1.67  | 1.10                                | 1.58                                | 0.15                         |
| 31  | Boreal flood plains and terraces with discontinuous permafrost, wet                   | 2.65  | 1.45  | 1.38                                | 1.44                                | 0.20                         |
| 32  | Boreal schist lower mountain slopes with continuous permafrost                        | 2.29  | 1.81  | 1.11                                | 1.60                                | 0.12                         |
| 33  | Boreal schist flood plains with discontinuous permafrost                              | 2.48  | 1.62  | 1.47                                | 1.49                                | 0.16                         |
| 34  | Boreal and subalpine schist mountain valleys  | 2.29  | 1.80  | 1.57                                | 1.78                                | 0.12                         |
| 35  | Boreal schist flood plains and terraces   | 2.18  | 1.92  | 1.78                                | 1.90                                | 0.10                         |
| 36  | Boreal terraces with discontinuous permafrost   | 2.10  | 2.0   | 1.48                                | 1.52                                | 0.10                         |
| 37  | Alpine plains and drainages with continuous permafrost                                | 2.45  | 1.65  | 0.97                                | 1.43                                | 0.15                         |
| 38  | Boreal terraces and high flood plains with continuous permafrost                      | 2.40  | 1.70  | 0.90                                | 1.44                                | 0.14                         |
| 39  | Boreal mica-rich terraces and flood plains with discontinuous permafrost              | 2.46  | 1.63  | 0.98                                | 1.02                                | 0.16                         |
| 40  | Alpine schist mountains with discontinuous permafrost                                 | 2.14  | 1.96  | 1.65                                | 1.82                                | 0.08                         |
| 41  | Boreal flood plains with discontinuous permafrost                                     | 2.34  | 1.76  | 1.33                                | 1.33                                | 0.13                         |
| 42  | Alpine low mountains with discontinuous permafrost, Nenana gravels                    | 2.36  | 1.73  | 1.34                                | 1.76                                | 0.13                         |
| 43  | Nonvegetated alluvium, Yukon-Kuskokwim bottomlands                                    | 2.34  | 1.76  | 1.39                                | 1.23                                | 0.13                         |
| 44  | Alpine plateaus and mountain summits with discontinuous permafrost, Nenana gravels    | 2.42  | 1.68  | 1.32                                | 1.82                                | 0.15                         |
| 45  | Subalpine and alpine plateau escarpments with discontinuous permafrost                | 2.36  | 1.73  | 1.44                                | 1.53                                | 0.13                         |
| 46  | Alpine and subalpine schist lower mountain slopes with discontinuous permafrost, cool | 2.28  | 1.80  | 1.12                                | 1.44                                | 0.11                         |
| 47  | Alpine schist mountains   | 2.14  | 1.96  | 1.70                                | 1.86                                | 0.08                         |

| No. | Landtype association  | Thawed heat capacity (MJ/m <sup>3</sup> .K) | Frozen heat capacity (MJ/m <sup>3</sup> .K) | Thawed thermal conductivity (W/m.K) | Frozen thermal conductivity (W/m.K) | Volumetric water content (%) |
|-----|---|---|---|-------------------------------------|-------------------------------------|------------------------------|
| 48  | Alpine and subalpine plateau summits  | 2.42  | 1.68  | 1.32                                | 1.82                                | 0.15                         |
| 49  | Boreal and alpine till plains with continuous permafrost                        | 2.31  | 1.79  | 1.42                                | 1.92                                | 0.12                         |
| 50  | Nonvegetated mountains, Alaska mountains  | 2.14  | 1.96  | 1.75                                | 1.97                                | 0.08                         |
| 51  | Nonvegetated alluvium, Alaska Mountains, Boreal                                 | 2.29  | 1.80  | 1.57                                | 1.78                                | 0.12                         |
| 52  | Boreal flood plains and terraces  | 2.21  | 1.89  | 1.90                                | 1.99                                | 0.10                         |
| 53  | Alpine schist terraces and mountain toeslopes with discontinuous permafrost     | 2.30  | 1.79  | 1.09                                | 1.64                                | 0.12                         |
| 54  | Boreal and alpine escarpments   | 2.36  | 1.73  | 1.44                                | 1.53                                | 0.13                         |
| 55  | Alpine schist alluvial fans with discontinuous permafrost                       | 2.07  | 2.03  | 1.70                                | 1.86                                | 0.10                         |
| 56  | Boreal flood plains and terraces with discontinuous permafrost                  | 2.34  | 1.76  | 1.39                                | 1.23                                | 0.13                         |
| 57  | Boreal fans and mountain footslopes   | 2.67  | 1.43  | 1.55                                | 1.70                                | 0.21                         |
| 58  | Boreal and alpine till plains and hills with discontinuous permafrost           | 2.38  | 1.72  | 1.13                                | 1.13                                | 0.14                         |
| 59  | Alpine and subalpine schist lower mountain slopes with discontinuous permafrost | 2.32  | 1.78  | 1.17                                | 1.71                                | 0.12                         |
| 60  | Alpine schist lower mountain slopes with discontinuous permafrost, Warm         | 2.28  | 1.81  | 1.12                                | 1.44                                | 0.11                         |
| 61  | Boreal glaciated lower mountain slopes  | 2.62  | 1.48  | 1.37                                | 1.54                                | 0.19                         |
| 62  | Boreal mid to high level flood plains   | 2.10  | 2.00  | 1.45                                | 1.46                                | 0.10                         |
| 63  | Alpine flood plains   | 2.17  | 1.93  | 1.86                                | 1.93                                | 0.10                         |
| 64  | Boreal schist alluvial fans   | 2.42  | 1.68  | 1.48                                | 1.56                                | 0.15                         |
| 65  | Alpine plains and hills with discontinuous permafrost, Nenana Gravels           | 2.10  | 2.0   | 1.67                                | 1.86                                | 0.07                         |
| 66  | Boreal glaciated plains and hills with discontinuous permafrost                 | 2.38  | 1.72  | 1.48                                | 1.71                                | 0.14                         |
| 67  | Boreal glaciated plains and hills   | 2.07  | 2.03  | 1.57                                | 1.82                                | 0.10                         |
| 68  | Alpine till plains with discontinuous permafrost                                | 2.31  | 1.79  | 1.42                                | 1.92                                | 0.12                         |
| 69  | Boreal lower mountain slopes with continuous permafrost                         | 2.41  | 1.69  | 1.14                                | 1.63                                | 0.14                         |
| 70  | Alpine terraces   | 2.07  | 2.03  | 1.99                                | 2.10                                | 0.06                         |
| 71  | Boreal wet meadows and bogs   | 2.58  | 1.52  | 1.09                                | 1.18                                | 0.19                         |
| 72  | Boreal loess footslopes and gravelly colluvial hills with continuous permafrost | 2.47  | 1.63  | 0.83                                | 1.31                                | 0.16                         |
| 73  | Alpine glaciated plains and hills with discontinuous permafrost                 | 2.07  | 2.03  | 1.57                                | 1.83                                | 0.06                         |

| No. | Landtype association   | Thawed heat capacity (MJ/m <sup>3</sup> .K) | Frozen heat capacity (MJ/m <sup>3</sup> .K) | Thawed thermal conductivity (W/m.K) | Frozen thermal conductivity (W/m.K) | Volumetric water content (%) |
|-----|--|---|---|-------------------------------------|-------------------------------------|------------------------------|
| 74  | Alpine glaciated mountains with discontinuous permafrost                 | 2.31  | 1.79  | 1.42                                | 1.92                                | 0.12                         |
| 75  | Alpine glaciated low mountain summits                                    | 2.37  | 1.73  | 1.33                                | 1.55                                | 0.14                         |
| 76  | Alpine glaciated low mountains with discontinuous permafrost             | 2.37  | 1.73  | 1.33                                | 1.55                                | 0.14                         |
| 77  | Boreal colluvial hill footslopes with continuous permafrost              | 2.56  | 1.54  | 0.79                                | 1.30                                | 0.18                         |
| 78  | Alpine and subalpine glaciated mountains with discontinuous permafrost   | 2.61  | 1.49  | 1.42                                | 1.71                                | 0.19                         |
| 79  | Alpine mixed lithology mountains   | 2.32  | 1.77  | 1.23                                | 1.45                                | 0.12                         |
| 80  | Alpine glaciated mountains with discontinuous permafrost, high elevation | 2.36  | 1.73  | 1.51                                | 1.68                                | 0.13                         |
| 81  | Alpine Diorite Terraces and flood plains                                 | 2.07  | 2.03  | 2.09                                | 2.23                                | 0.06                         |
| 82  | Alpine lower mountain slopes and fans with discontinuous permafrost      | 2.07  | 2.03  | 1.99                                | 2.10                                | 0.06                         |
| 83  | Alpine mixed lithology mountains, high elevation                         | 2.32  | 1.77  | 1.23                                | 1.45                                | 0.12                         |
| 84  | Alpine low schist mountains with discontinuous permafrost                | 2.08  | 2.02  | 1.31                                | 1.77                                | 0.06                         |
| 85  | Alpine Fans  | 2.19  | 1.91  | 1.81                                | 2.06                                | 0.10                         |
| 86  | Alpine dark sedimentary mountains  | 2.08  | 2.02  | 1.82                                | 1.92                                | 0.07                         |
| 87  | Alpine dark sedimentary mountains, High elevation                        | 2.08  | 2.02  | 1.85                                | 2.05                                | 0.07                         |
| 88  | Alpine and subalpine mountains   | 2.08  | 2.02  | 1.75                                | 1.88                                | 0.07                         |
| 89  | Alpine plains and hills with continuous permafrost, Nenana gravels       | 2.45  | 1.65  | 0.97                                | 1.43                                | 0.15                         |
| 90  | Boreal loess plains and peat plateaus with continuous permafrost         | 2.34  | 1.76  | 0.97                                | 1.39                                | 0.13                         |
| 91  | Alpine till plains and hills with discontinuous permafrost               | 2.38  | 1.72  | 1.26                                | 1.63                                | 0.14                         |
| 92  | Nonvegetated alluvium, Alaska mountains, Alpine                          | 2.14  | 1.96  | 1.70                                | 1.86                                | 0.08                         |
| 93  | Alpine schist flood plains and terraces                                  | 2.18  | 1.92  | 1.75                                | 1.94                                | 0.09                         |
| 94  | Subalpine mountains  | 2.13  | 1.96  | 1.66                                | 1.77                                | 0.08                         |
| 95  | Alpine Mountain Fans   | 2.06  | 2.04  | 1.87                                | 2.03                                | 0.06                         |
| 96  | Alpine backslopes on hills, Nenana gravels                               | 2.40  | 1.72  | 1.50                                | 1.65                                | 0.14                         |
| 97  | Boreal loess plains, hills, and drains with continuous permafrost        | 2.34  | 1.76  | 0.97                                | 1.39                                | 0.13                         |
| 98  | Alpine and boreal alluvial fans  | 2.07  | 2.03  | 1.99                                | 2.10                                | 0.10                         |

| No. | Landtype association   | Thawed heat capacity (MJ/m <sup>3</sup> .K) | Frozen heat capacity (MJ/m <sup>3</sup> .K) | Thawed thermal conductivity (W/m.K) | Frozen thermal conductivity (W/m.K) | Volumetric water content (%) |
|-----|--|---|---|-------------------------------------|-------------------------------------|------------------------------|
| 99  | Alpine glaciated mountain summits and benches with discontinuous permafrost      | 2.37  | 1.73  | 1.33                                | 1.55                                | 0.14                         |
| 100 | Alpine terraces and outwash plains with continuous permafrost                    | 2.47  | 1.63  | 0.90                                | 1.35                                | 0.16                         |
| 101 | Alpine fans with discontinuous permafrost  | 2.06  | 2.04  | 1.87                                | 2.07                                | 0.06                         |
| 102 | Boreal and alpine hills with discontinuous permafrost                            | 2.38  | 1.72  | 1.26                                | 1.63                                | 0.14                         |
| 103 | Alpine low schist mountain summits with continuous permafrost                    | 2.28  | 1.81  | 1.12                                | 1.44                                | 0.11                         |
| 104 | Alpine Recent Moraines   | 2.31  | 1.79  | 1.62                                | 1.72                                | 0.12                         |
| 105 | Alpine glaciated lower mountain slopes   | 2.47  | 1.63  | 1.37                                | 1.47                                | 0.16                         |
| 106 | Boreal outwash plains and fans with discontinuous permafrost                     | 2.10  | 1.99  | 1.93                                | 2.04                                | 0.10                         |
| 107 | Alpine Till plains and hills   | 2.47  | 1.63  | 1.37                                | 1.47                                | 0.16                         |
| 108 | Alpine glaciated mountains with discontinuous permafrost, cool                   | 2.51  | 1.59  | 1.18                                | 1.64                                | 0.17                         |
| 109 | Boreal Diorite flood plains  | 2.16  | 1.93  | 2.05                                | 2.14                                | 0.10                         |
| 110 | Alpine glaciated Diorite plains and hills  | 2.38  | 1.72  | 1.30                                | 1.54                                | 0.14                         |
| 111 | Alpine lower mountain colluvial slopes   | 2.23  | 1.87  | 1.57                                | 1.66                                | 0.10                         |
| 112 | Alpine diorite mountains, Interior   | 2.32  | 1.77  | 1.38                                | 1.56                                | 0.12                         |
| 113 | Boreal plains with continuous permafrost   | 2.94  | 1.16  | 0.98                                | 1.46                                | 0.27                         |
| 114 | Alpine and subalpine glaciated mountain backslopes                               | 2.47  | 1.63  | 1.37                                | 1.47                                | 0.16                         |
| 115 | Alpine glaciated low Diorite mountains with discontinuous permafrost             | 2.08  | 2.02  | 1.79                                | 2.11                                | 0.07                         |
| 116 | Alpine Diorite mountains with discontinuous permafrost                           | 2.32  | 1.77  | 1.38                                | 1.64                                | 0.12                         |
| 117 | Nonvegetated alluvium, Cook Inlet Lowlands                                       | 2.23  | 1.87  | 1.53                                | 1.56                                | 0.10                         |
| 118 | Subalpine Fans   | 2.09  | 2.01  | 1.66                                | 1.69                                | 0.10                         |
| 119 | Alpine alluvial fans   | 2.39  | 1.70  | 1.67                                | 1.71                                | 0.14                         |
| 120 | Alpine Diorite Fans  | 2.34  | 1.76  | 1.36                                | 1.59                                | 0.13                         |
| 121 | Boreal flood plains, Dry   | 2.14  | 1.96  | 1.59                                | 1.61                                | 0.08                         |
| 122 | Boreal outwash plains with continuous permafrost                                 | 2.46  | 1.64  | 1.26                                | 1.77                                | 0.16                         |
| 123 | Alpine and subalpine Diorite fans and flood plains with discontinuous permafrost | 2.07  | 2.03  | 2.09                                | 2.23                                | 0.06                         |
| 124 | Boreal Fans  | 2.19  | 1.91  | 1.37                                | 1.40                                | 0.10                         |
| 125 | Boreal and subalpine lower mountain slopes                                       | 2.47  | 1.63  | 1.32                                | 1.43                                | 0.16                         |

| No. | Landtype association  | Thawed heat capacity (MJ/m <sup>3</sup> .K) | Frozen heat capacity (MJ/m <sup>3</sup> .K) | Thawed thermal conductivity (W/m.K) | Frozen thermal conductivity (W/m.K) | Volumetric water content (%) |
|-----|---|---|---|-------------------------------------|-------------------------------------|------------------------------|
| 126 | Alpine low mountains  | 2.32  | 1.78  | 1.60                                | 1.71                                | 0.12                         |
| 127 | Alpine fans and flood plains, High elevation                            | 2.00  | 2.10  | 1.86                                | 1.99                                | 0.05                         |
| 128 | Boreal glaciated hills and plains                                       | 2.47  | 1.63  | 1.32                                | 1.43                                | 0.16                         |
| 129 | Alpine mountains  | 2.04  | 2.06  | 1.86                                | 1.98                                | 0.06                         |
| 130 | Nonvegetated mountains, south central mountains                         | 2.04  | 2.06  | 1.86                                | 1.98                                | 0.06                         |
| 131 | Alpine recent moraines, Diorite   | 1.99  | 2.11  | 1.84                                | 1.90                                | 0.04                         |
| 132 | Subalpine and alpine Diorite flood plains                               | 2.14  | 1.96  | 1.93                                | 1.95                                | 0.08                         |
| 133 | Alpine cirque valleys   | 2.54  | 1.56  | 1.41                                | 1.55                                | 0.18                         |
| 134 | Alpine schist lower mountain slopes with discontinuous permafrost       | 2.31  | 1.79  | 1.18                                | 1.63                                | 0.12                         |
| 135 | Alpine schist mountains, high elevation                                 | 2.14  | 1.96  | 1.75                                | 1.97                                | 0.08                         |
| 136 | Alpine Diorite mountains  | 2.19  | 2.30  | 1.58                                | 1.64                                | 0.09                         |
| 137 | Subalpine mountain colluvial slopes                                     | 2.20  | 1.89  | 1.61                                | 1.66                                | 0.10                         |
| 138 | Alpine, subalpine, and Boreal recent moraines                           | 2.32  | 1.78  | 1.26                                | 1.31                                | 0.12                         |
| 139 | Alpine Diorite flood plains and wet mountain toeslopes                  | 2.14  | 1.96  | 1.94                                | 1.97                                | 0.08                         |
| 140 | Alpine diorite cirque valleys   | 2.54  | 1.56  | 1.41                                | 1.55                                | 0.18                         |
| 141 | Subalpine glaciated mountains   | 2.63  | 1.47  | 1.39                                | 1.49                                | 0.20                         |
| 142 | Boreal flood plains   | 2.19  | 1.91  | 1.37                                | 1.41                                | 0.10                         |
| 143 | Subalpine glaciated benches on lower mountain slopes                    | 2.63  | 1.47  | 1.39                                | 1.49                                | 0.20                         |
| 144 | Boreal bogs   | 3.27  | 0.83  | 0.30                                | 0.93                                | 0.35                         |
| 145 | Boreal flood plains and terraces, Wet                                   | 2.23  | 1.87  | 1.53                                | 1.56                                | 0.10                         |
| 146 | Boreal flood plains, Very Wet   | 2.90  | 1.19  | 0.70                                | 1.18                                | 0.26                         |
| 147 | Subalpine and alpine glaciated benches on lower mountain slopes         | 2.63  | 1.47  | 1.39                                | 1.49                                | 0.20                         |
| 148 | Subalpine glaciated lower mountain backslopes                           | 2.20  | 1.90  | 1.61                                | 1.66                                | 0.10                         |
| 149 | Boreal mica-rich mountain toeslopes with continuous permafrost          | 2.56  | 1.54  | 0.73                                | 1.21                                | 0.18                         |
| 150 | Boreal mountain toeslopes with discontinuous permafrost, Nenana gravels | 2.38  | 1.72  | 1.11                                | 1.65                                | 0.14                         |
| 151 | Boreal terraces and flood plains with discontinuous permafrost          | 2.40  | 1.70  | 0.91                                | 1.44                                | 0.14                         |

**Table A3.** Nine snow classes identified within DENA are used as snow input to the model. The snow classes are identified by integrating the snow class from Sturm et al. (1995) with ecotypes from North America Land Cover Characteristics Data Base Version 2.0 (Loveland et al. 1999).

| <b>Class no.</b> | <b>Class name</b> | <b>Density of fresh snow (kg/m<sup>3</sup>)</b> | <b>Maximum density of snow (kg/m<sup>3</sup>)</b> |
|------------------|-------------------|---|---|
| 1                | Bare surface      | 80  | 320   |
| 2                | Upland tundra     | 65  | 180   |
| 3                | Alpine            | 100   | 320   |
| 4                | Inland water      | 65  | 185   |
| 5                | Shrub deciduous   | 70  | 220   |
| 6                | Grassland         | 100   | 280   |
| 7                | Mixed shrub       | 140   | 420   |
| 8                | Conifer forest    | 70  | 220   |
| 9                | Mixed forest      | 90  | 180   |

## Appendix B. The GIPL Model for Estimation of Temporal and Spatial Variability of the Active-Layer Thickness and Mean Annual Ground Temperatures

Sergey S. Marchenko and Vladimir E. Romanovsky

The Geophysical Institute Permafrost Lab (GIPL) model was developed specifically to assess the effect of a changing climate on permafrost. The GIPL 1.0 model is a quasi-transitional, spatially distributed, equilibrium model for calculating the active-layer thickness and mean annual ground temperature. It accounts effectively for the effects of snow cover, vegetation, soil moisture, and soil thermal properties. It allows for the calculation of maximum active-layer thickness (ALT) and mean annual ground temperatures (MAGT) at the bottom of the active layer. Our approach to determine the ALT and MAGT is based on an approximate analytical solution that includes freezing/thawing processes and provides an estimation of thermal offset due to the difference in frozen and thawed soil thermal properties (Kudryavtsev et al. 1974). It uses the idea of applying the Fourier temperature wave propagation theory to a medium with phase transitions, such as freezing/thawing ground. Application of this approach resulted in the discovery of the thermal offset and an understanding of the laws that govern the dynamics of the ground thermal regime. These discoveries led to an understanding of the effects that the thermal properties of the ground have upon the MAGT and ALT, and how periodically (seasonally) varying climatic parameters affect permafrost dynamics. The output parameters of this method are given as annual averages. Input and output parameters are listed in Table B1. The effect of geothermal heat flux is ignored because it is considered to have a minimal impact on the MAGT and ALT values. For the areas with permafrost, the MAGT is the same as a mean annual temperature at the permafrost table (upper surface of permafrost). Where permafrost is absent, the MAGT is the mean annual temperature at the bottom of seasonally-frozen layer.

**Table B1.** Model input and output variables.

| <b>Input Variables</b>                                   | <b>Notation</b> | <b>Units</b> |
|--|-----------------|--------------|
| Seasonal range of air temperature variations (amplitude) | $A_a$           | °C           |
| Mean annual air temperature                              | $T_a$           | °C           |
| Snow Water Equivalent                                    | SWE             | m            |
| Height of vegetation cover                               | $H_v$           | m            |
| Thermal diffusivity of vegetation in frozen state        | $D_{vf}$        | $m^2/s$      |
| Thermal diffusivity of vegetation in thawed state        | $D_{vt}$        | $m^2/s$      |
| Thermal conductivity of frozen soil                      | $K_f$           | W/(m*K)      |

| <b>Input Variables</b>   | <b>Notation</b> | <b>Units</b>       |
|--|-----------------|--------------------|
| Thermal conductivity of thawed soil  | $K_{th}$        | W/(m*K)            |
| Volumetric water content   | VWC             | Fraction of 1      |
| Volumetric latent heat of ice fusion   | 334e6           | J/m <sup>3</sup>   |
| Volumetric heat capacity of snow cover                                       | $C_{sn}$        | J/m <sup>3</sup> K |
| Volumetric heat capacity of thawed ground                                    | $C_{th}$        | J/m <sup>3</sup> K |
| Volumetric heat capacity of frozen ground                                    | $C_f$           | J/m <sup>3</sup> K |
| <b>Output Variables</b>  | <b>Notation</b> |                    |
| Correction to air temperature accounting for snow cover effect, °C           | $\Delta T_{sn}$ |                    |
| Correction to air temperature amplitude accounting for snow cover effect, °C | $\Delta A_{sn}$ |                    |
| Correction to air temperature accounting for vegetation cover , °C           | $\Delta T_v$    |                    |
| Correction to air temperature amplitude accounting for vegetation cover , °C | $\Delta A_v$    |                    |
| Seasonal range of temperature variations at the ground surface, °C           | $A_{gs}$        |                    |
| Mean annual temperatures at the ground surface, °C                           | $T_{gs}$        |                    |
| Snow density, kg/m <sup>3</sup>  | $\rho_{sn}$     |                    |
| Snow thermal conductivity, W/(m*K)   | $K_{sn}$        |                    |
| Thermal offset, °C   | $\Delta T_k$    |                    |
| Mean annual soil surface temperature, °C                                     | MAGST           |                    |
| Mean annual soil temperature at the bottom of ALT , °C                       | MAGT            |                    |
| Active-layer thickness, m  | ALT             |                    |

### **Mean Annual Ground Temperature at the Bottom of the Active Layer**

Throughout the years, simplified analytical solutions for temperature modeling in the ALT have been applied for structural engineering and other practical purposes. Most of these methods have been based on the Stefan solutions, and they do not yield a good level of accuracy (Romanovsky and Osterkamp 1997). It was determined that the best method for computation of the ALT and MAGT

was a modified version of Kudryavtsev’s approach (Romanovsky and Osterkamp 1997). This approach is the core of the GIPL 1.0 model, which treats the complex system including air, snow cover, surface vegetation, and active layer, as a set of individual layers with different thermal properties (Figure B1). In the regions of Alaska and East-Siberia that were analyzed, surface vegetation consists of lichens, grass, and moss (sphagnum or feather mosses) (Brown and Kreig 1983, Feldman et al. 1988). The upper level of vegetation consisting of trees and shrubs is not considered in the model. This upper level vegetation affects the thickness and density of the snow cover, along with the amount of solar radiation reaching the ground surface. The model takes into account only low-level vegetation (surface vegetation) that is less than 0.5 meter high, because the information about higher vegetation such as trees and tall shrubs is already incorporated into the monthly surface air temperature data, which were used as input data in the model.

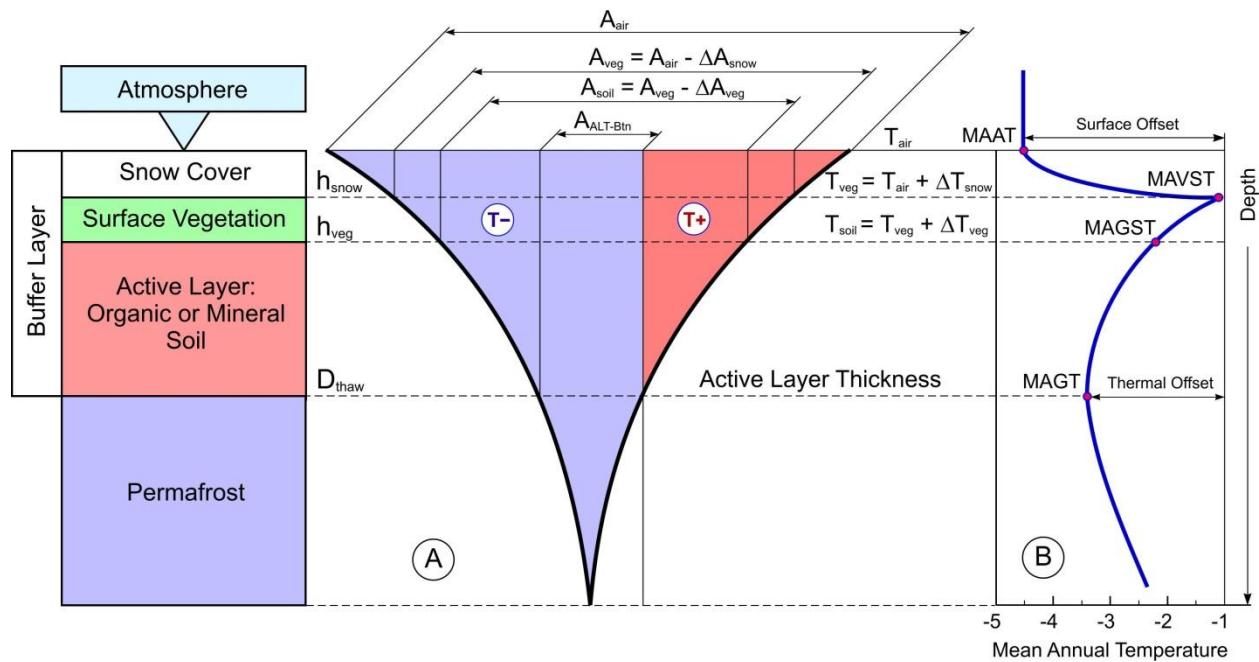


**Figure B1.** The GIPL 1.0 model conceptual diagram (A) and schematic profile of mean annual temperature through the lower atmosphere, active layer and upper permafrost (B). Acronyms: MAAT (Mean Annual Air Temperature), MAGST (Mean Annual Ground Surface Temperature), MAGT (Mean Annual Ground Temperature), ALT (Active-Layer Thickness).

Snow cover plays an important role in heat exchange processes between the surface of the ground and the atmosphere. The warming effect of the snow cover has been calculated using approximate formulas derived by A. Lachenbruch (1959) and V. Romanovsky (1987), which incorporate ground properties, vegetation cover, and their respective effect on heat turnovers through the snow. Heat turnovers are defined as the quantity of incident heat (during the heating period), or out-going heat (during the cooling period) throughout the media over a given time interval (usually half year

increments). Thus, the heat turnover is  $Q = \int_{t_1}^{t_2} q(t)dt$ , where  $t_1$  and  $t_2$  are the times when the regime

changes from ground heating to ground cooling, or from cooling to heating periods, and  $q(t)$  is the heat flux through the ground surface as a function of time.

Our model takes into account only conductive heat transfer through the surface vegetation (lichens, moss, and grasses). The rate of heat turnover between the ground and atmosphere has been shown to have a strong dependence on vegetation cover. In summer, surface vegetation prevents solar radiation from penetrating into the ground and warming it. In wintertime, surface vegetation acts as an insulator and keeps heat in the ground.

The seasonal freezing and thawing cycles cause changes in the thermal properties of soils within the active layer. Typically, this effect leads to a decrease in MAGTs with depth within the active layer. The thermal offset is defined as the difference between the mean annual temperature MAGT at the bottom of the active layer and the mean annual temperature at the ground surface (Kudryavtsev et al. 1974, Goodrich 1978, Burn and Smith 1988). The thermal offset depends on soil moisture content and thermal properties, and has the most pronounced effect within a peat layer (Marchenko and Romanovsky 2007). The analytical equation to estimate the thermal offset was given by Kudryavtsev (1981) (no derivation was published), and was formally derived by V. Romanovsky (Romanovsky and Osterkamp 1995).

The approach to simulate MAGT in the GIPL 1.0 model is the consecutive layer-by-layer introduction of thermal effects of snow, ground surface vegetation, and the soils within the active layer on mean annual temperatures and seasonal amplitudes at each considered level (snow surface, vegetation surface, and ground and permafrost table). However, this scheme is not totally additive because the estimation of the impact of each new layer already includes the thermal effects of all layers above it. Moreover, in this approach, the thermal effect of snow reflects the thermal properties and temperature field dynamics in the subsurface layers through the heat turnover estimation. As a result, this approach takes into account some negative and positive feedbacks between designated layers in the “atmosphere-permafrost” system.

### **The Active-Layer Thickness**

Calculation of the ALT is the final step in the GIPL 1.0 model (Romanovsky and Osterkamp 1997). The formula was derived for homogeneous ground, but in actuality, even if the soil properties are the same throughout the active layer, the moisture content or mode of heat flow may vary significantly. This can make the active layer inhomogeneous with regard to its thermal properties. Also, the model does not take into account unfrozen water, which can exist in the frozen active layer even at temperatures below zero Celsius, and has a significant effect on the ground’s thermal properties (Williams 1964, Williams and Smith 1989). The assumption of a periodically steady state temperature regime seems to be a good approximation when applied to the annual temperature cycle, which varies from year to year (Romanovsky and Osterkamp 1997). Considering the advantages along with the shortcomings, the GIPL 1.0 model appears to give a good representation of the coupling between permafrost and the atmosphere. When applied to long-term (decadal and longer time scale) averages, this approach shows an accuracy of +0.2-0.4°C for the mean annual ground temperatures and +0.1 – 0.3 m for the active-layer thickness calculations (Sazonova and Romanovsky 2003). The relative errors do not exceed 32% for the ALT calculations, but typically they are between 10 and 25%. The differences in 0.2-0.4°C between calculated and measured mean annual ground temperatures were obtained for the long-term multi-year average estimations.

## The Input Dataset

At the present stage of development, the GIPL 1.0 model is combined with ArcGIS to facilitate preparation of input parameters (climate forcing from observations or from Global or Regional Climate Models) and visualization of simulated results in a form of digital maps (Figure B2).

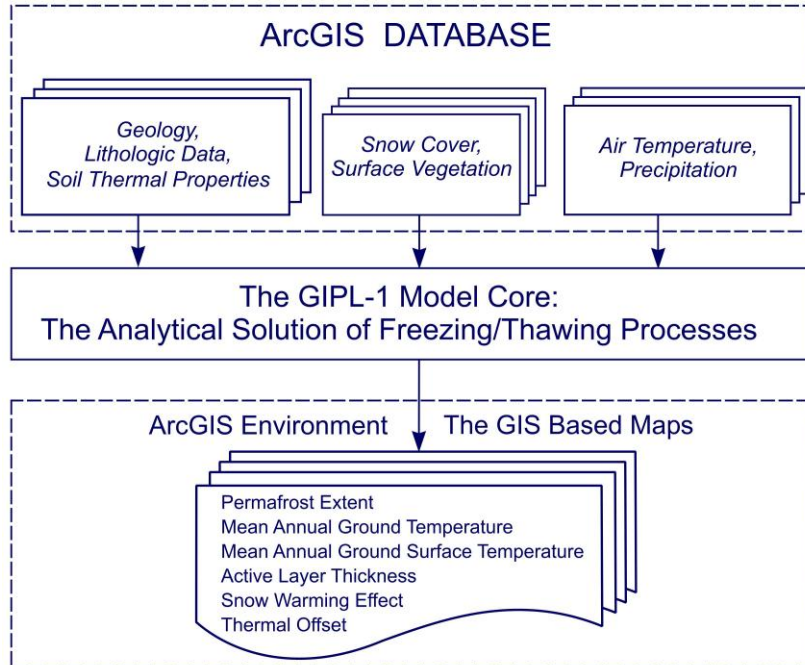


**Figure B2.** A schematic representation of integration of GIS with GIPL 1.0 model.

## Literature Cited

- Brown, J., and R. A. Kreig. 1983. Guidebook to permafrost and related features along the Elliot and Dalton highways, Fox to Prudhoe Bay, Alaska. Proceedings of Fourth International Conference on Permafrost. 18–22 July 1983, University of Alaska, Fairbanks, Alaska Division of Geological and Geophysical Surveys, 230 pp.
- Burn, C. R., and C. A. S. Smith. 1988. Observations of the ‘thermal offset’ in near-surface MAGTs at several sites near Mayo, Yukon Territory, Canada. *Arctic* 41(2):99–104.
- Feldman, G. M., A. S. Tetelbaum, N. I. Shender, and R. I. Gavriliev. 1988. The guidebook for temperature regime forecast in Yakutia (in Russian), Yakutsk, 240 pp.
- Goodrich, L. E. 1978. Some results of numerical study of ground thermal regime. Proceedings of the Third International Conference on Permafrost. National Research Council of Canada, Ottawa, vol.1:29–34.
- Kudryavtsev, V. A. (editor). 1981. Permafrost (short edition) (in Russian), MSU Press, 240 pp.

- Kudryavtsev, V. A., L. S. Garagula, K. A. Kondrat'yeva, and V. G. Melamed. 1974. Osnovy merzlotnogo prognoza (in Russian). MGU Press, 431 pp. [CRREL Translation: V. A. Kudryavtsev et al. 1977. Fundamentals of frost forecasting in geological engineering investigations, CRREL Draft Translation 606, 489 pp.]
- Lachenbruch, A. H. 1959. Periodic heat flow in a stratified medium with application to permafrost problems. US Geological Survey Bulletin, 1083-A, 36 pp.
- Marchenko, S., and V. E. Romanovsky. 2007. Modeling the effect of organic layer and water content on permafrost dynamics in the northern hemisphere. Eos, Transactions, American Geophysical Unions, 88(52), Fall Meet. Suppl., GC23A-0985.
- Romanovsky, V. E. 1987. Approximate calculation of the insulation effect of the snow cover. Geokriologicheskije Issledovania (in Russian), MGU Press, vol. 23, 145–157.
- Romanovsky, V. E., and T. E. Osterkamp. 1995. Interannual variations of the thermal regime of the active layer and near-surface permafrost in Northern Alaska. Permafrost and Periglacial Processes 6(4):31–335.
- Romanovsky, V. E., and T. E. Osterkamp. 1997. Thawing of the active layer on the coastal plain of the Alaskan Arctic. Permafrost and Periglacial Processes 8(1):1–22.
- Sazonova, T. S., and V. E. Romanovsky. 2003. A model for regional-scale estimation of temporal and spatial variability of active layer thickness and mean annual ground temperatures. Permafrost and Periglacial Processes 14:125–139.
- Williams, P. J. 1964. Unfrozen water content of frozen soils and soil moisture suction. Geotechnique 14(3):231–246.

The Department of the Interior protects and manages the nation's natural resources and cultural heritage; provides scientific and other information about those resources; and honors its special responsibilities to American Indians, Alaska Natives, and affiliated Island Communities.

NPS 953/124187, March 2014

**National Park Service**  
**U.S. Department of the Interior**



---

**Natural Resource Stewardship and Science**

1201 Oakridge Drive, Suite 150  
Fort Collins, CO 80525

[www.nature.nps.gov](http://www.nature.nps.gov)

**EXPERIENCE YOUR AMERICA™**